CHAPTER 1: INTRODUCTION

Alcoholic Liver Disease (ALD) is one of the main causes of mortality across the globe and is a major health concern. Liver diseases are the fifth most common cause of deaths. Prolonged alcohol abuse causes liver diseases ranging from early to late stages including mild steatosis, steatohepatitis, inflammation, fibrosis and cirrhosis (Fullwood, 2014 #627) . Reportedly there is a 15% probability that alcoholic cirrhotic patients develop liver cancer (Yip & Burt, 2006).

'Saponin' is a Latin word for soap which is being given to it as it has been used as soap for centuries. They have been a constituent of many plant drugs and folk medicines. Saponins form foams in water, have hemolytic, anti-microbial, anti-cancerous and anti-inflammatory activity, bitter taste and are toxic to fish (Güçlü-Üstündağ & Mazza, 2007).

Saponins occur in a wide variety of plants including roots of *Salvia officinalis*, *Panax notoginseng* and stems of *Cortex albiziae*, *Cryptocarya foetida*, *Cimcifuga simplex*, *Entada pursaetha*, *Catunaregam spinosa*, *Corchorus depressus* etc (Vincken et al., 2007). The saponins are obtained from the methanolic plant extract after a series of steps and are confirmed by thin liquid chromatography (Vincken, Heng, de Groot, & Gruppen, 2007). Changkil saponins extracted from the root of *Platycodon grandiflorum* reportedly prevent acute liver injury induced by ethanol by blocking bioactivation of ethanol and its free radical scavenging effects (Khanal et al., 2009).

Nanotechnology has been found useful in the detection, diagnosis and treatment of a number of diseases. Nanoparticles (Nps) are widely used in biological and pharmaceutical fields (Alivisatos, 2004). The nanoparticles are widely employed in the targeted drug delivery because of their small sizes. Metallic Nps are reported respond resonantly to a time-varying magnetic field causing transfer of energy to the particles (Pissuwan, Valenzuela, & Cortie, 2006).

Gold nanoparticles (AuNps) are in use since the ancient times but it was assumed earlier that the color of the nanoparticles is because of the chemicals used in their preparation; however in 1857 Michael Faraday prepared colloidal gold particles and discovered that the solution color is due to the size of the gold particles (Wulf, 2012). AuNps have been prepared chemically and by green synthesis. Green synthesis is more reliable as it does not involve hazardous chemicals and is environment friendly (Khanal, Choi, Hwang, Chung, & Jeong, 2009). Recently, the anti-angiogenic property of AuNps have been discovered (Ghosh, Han, De, Kim, & Rotello, 2008) (Rosarin & Mirunalini, 2011).

The constituents of nanoparticles should be biocompatible and biodegradeable to be excreted via bile and kidneys. In the case of nanospheres/nanoparticles the drug is dispersed throughout the particles while in nanocapsules it is confined to a cavity surrounded by a polymeric membrane (Burda, Chen, Narayanan, & El-Sayed, 2005). Various plant extracts have been employed in treatment, saponins have also been studied pharmaceutically and their anti-inflammatory, anti-cancerous etc properties (Lasagna-Reeves et al., 2010). Accumulation of gold nanoparticles (AuNps) in the body by repeated administrations can reach to toxic levels so in order to improve the biocompatibility of AuNps it is preferable to use non-toxic reagents (Lasagna-Reeves et al., 2010).

So far only limited research has been carried out on the green synthesis of gold nanoparticles using varying gold solution concentrations and molar ratios. Usually crude plant extracts are used in the synthesis process which does not support the results effectively. The current study focuses on the effect of change in concentrations and molar ratios on the particle size and stability. Surface Plasmon Resonance (SPR) is size dependant. The position of the SPR depends upon the shape of the particles e.g., the position of SPR band for gold nanorods is around 850 nm (Wulf, 2012). The increase in the ionic strength causes the aggregation of AuNps which leads to a red shift in the SPR band. The aggregated AuNps give blue color to the solution (Burda et al., 2005).

Since the change in synthesis conditions such as concentration and ratios affects the nanoparticle characteristics in the case of chemical synthesis, as reported earlier by Turkevich and Frens and latter by Kara and William (Zabetakis et al., 2012) , therefore it is important to check how these changes affect the nanoparticle characteristics in the case of green synthesis.

A comparison between effect with/ without (w/wo) treatment on CCl_4 and ethanol induced liver inflammation in mice is the focus of the current study. The study design is based on the hypothesis that saponin gold nanoparticles (SapAuNps) would be more efficient and effective in comparison to treatment with the purified saponins or in the absence of treatment. For this purpose a mouse inflammatory model is developed to be tested in all the three ways i.e., with the purified saponins, with the SapAuNps and without any of them.

CHAPTER 2: LITERATURE REVIEW

2.1 Selection of Animals for Liver Damage

Owing to the reasons such as the need to utilize large numbers of animals, expenditure, and stabling facilities rat and mice were preferred by the researchers to develop models of liver damage using toxin administration or bile duct ligation (BDL) (Hooijmans, Leenaars, & Ritskes-Hoitinga, 2010). Korpassy and Kovacs developed a rat model of cirrhosis by tannic acid administration about 60 years ago (Korpassy & Kovacs, 1949).

2.2 Effects of injury on the Liver

The study of liver damage includes blood tests, biopsy and noninvasive imaging techniques. Liver injury triggers an organized system of molecular changes which involve cellular activation of hepatic stellate cells which deposit large quantities of extracellular matrix (ECM) components within the liver causing fibrosis (Friedman, 2008; Gressner & Weiskirchen, 2006). If the injury is temporary, the changes are fleeting and fibrosis may resolve, however if the injury is persistent, chronic inflammation and accumulation of the ECM cause the substitution of normal liver parenchyma by scar tissue. The soluble mediators in the injured organ attract myofibroblasts which change the composition of the ECM in the injured tissue (Zeisberg et al., 2007).

2.3 Induction of Carbon Tetrachloride for Liver Injury

Carbon tetrachloride or other hepatotoxins have been used to induce chronic liver damage in wild-type and knock-out mice via the intragastric or intraperitoneal or subcutaneous routes of administration to study the pathogenesis of liver fibrosis (Abbate et al., 2008). It has been reported by Chang et al. that CCl_4 administration leads to a prompt liver damage in mice in comparison to other hepatotoxins (Chang, Yeh, Chang, & Chen, 2005).

The induction of multiple doses of carbon tetrachloride ($CC1_4$) either by subcutaneous or intraperitoneal routes or by inhalation is reported to cause chronic liver damage in the rat (Li, Wang, & Asahina, 2013).

Cameron and Karunaratne in 1936 stressed on the importance of extent of damage to the liver i.e., the damage must be confined within a narrow range to study the mechanisms properly. A new approach was proposed in which variation in the body weight was used as a measure of damage to the liver caused by intragastric administration of CCl_4. The adjustment in the doze of CCl_4 according to the weight change was successful in maintaining prolonged liver damage for studying late stage liver disease (Liedtke et al., 2013; McLean, McLean, & Sutton, 1969).

There are different routes to administer CCl_4 for inducing liver damage in mice including oral, subcutaneous, inhalation and intraperitoneal routes of administration. The oral route has been reported to cause early mortality in mice. The administration of CCl_4 via the subcutaneous route for a prolonged period of time leads to the extensive formation of granulomas at the site of injection and affects other remote organs such as the lungs (Ackermann et al., 2007) . Although the administration of CCl4 via inhalation does not affect other remote organs and induces liver injury within a short time frame, it is operator-dependent and inhalation for 2 mins can cause respiratory arrest mostly in mice (Vasina et al., 2012).

The administration of CCl_4 via the intraperitoneal route with phenobarbitol in drinking water has been proved to induce severe liver damage in C57BL/6NCrl mice (Liedtke et al., 2013). Although the intraperitoneal route of administration induces severe liver damage within a short time frame however sarcopenia, aggressiveness, and body weight loss are its associated risks which usually occur during the experimental period. Paraffin oil which is used as an agent to deliver CCl_4 is neutral in nature but the preparation of the CCl_4–paraffin mixture is not as easy as CCl_4 tends to evaporate owing to its volatile nature.

The mouse strains differ in their sensitivity to CCl_4 e.g., C57BL/6 mice develop less liver injury and fibrosis than BALB/c mice. Reportedly, IL-6 hepatic gene has an enhanced expression in mice receiving CCl_4 via the intraperitoneal route (Liedtke et al., 2013). The hepatocytes are reported to metabolize CCl_4 to toxic trichloromethyl (CCl_3) radicals, which stimulate massive centrilobular liver necrosis (Hooijmans et al., 2010). In addition to this CCl_4 induction is also known to cause apoptotic cell death of hepatocytes (Li et al., 2013).

2.4 Gold Nanoparticles

The term “nano” is coined by Greeks. It means small and is one billionth part (10-9) of matter. American Society for Testing and Materials (ASTM international 2006) has proposed that nanoparticles have two or more than two dimensions and their size lies in the range is of 1 – 100 nm (Alanazi, Radwan, & Alsarra, 2010). Owing to their small sizes the nanoparticles have better physicochemical properties in comparison to bulk gold and are therefore widely employed in the electronic, photochemical, biomedical and chemical fields (Kim & Jon, 2012). The hybrids formed by the combination of inorganic nanoparticles with organic materials are more useful because of their unique physical, chemical, optical and electrical properties.

Nanoparticles have also been used in imaging and therapies due to their easy modification, stability and high drug loading capacity (Pal, Panigrahi, Bhattacharyya, & Chakraborti, 2013). It has been found that the shape and size of the nanoparticles controls their magnetic, catalytic, electrical and optical properties. In the diverse field of biomedicine nanoparticles have wide applications such as to deliver pharmaceutics, for diagnostic and therapeutic purposes. Owing to their small sizes nanoparticles can be used for targeted drug delivery. The metallic nanoparticles have been used as hypothermic agents to kill the tumor cells by transfering toxic thermal energy generated by the phenomenon of magnetic resonance (Guo, Guo, Yuan, & Zeng, 2014).

The bulk gold is yellow solid and is inert in nature while the liquid gold nanoparticles have wine red color and are reported to be anti-oxidant. The properties of gold nanoparticles are determined by their inter particle interaction (Guo et al., 2014), their sizes range from 1 nm to 8 μm and they have different shapes such as spherical, sub-octahedral, octahedral, decahedral, icosahedral, irregular, tetrahedral, nanotriangles, hexagonal platelets , nanorods etc. The optical properties of triangular gold nanoparticles are better than the spherical nanoparticles.

The use of plant extract in the synthesis of gold nanoparticles is an important bio synthesis technique to investigate the medical uses of gold nanoparticles. The therapeutic effectiveness of gold nanoparticles in the form of radiations has also been investigated (Ganeshkumar et al., 2012). The various uses of gold nanoparticles include biomolecular detection, hypothermal destruction of cancer cells and labeling for cells and proteins.

Fluorescent gold nanoparticles aid in molecular imaging of many enzymes and metabolites which helps understand the cellular functions in cancer (Pal et al., 2013). The unique anisotropic geometry of gold nanorods is responsible for their remarkable absorption in both visible and near infrared (NIR) regions and renders them suitable for applications in the fields of biosensing, gene delivery and photo thermal therapy. Gold nanoparticles are preferred as molecular probes for X-ray CT imaging in comparison to conventional iodine-based agents because the absorption coefficient of gold is higher than iodine due to its higher atomic number and electron density which enables it to enhance the CT contrast more than iodine (Stobiecka & Hepel, 2011). Furthermore gold nanoparticles are non-cytotoxic and have a large surface area available for modification with targeting molecules or specific biomarkers (Guo et al., 2014).

The gold nanoparticles are able to bear high drug loads due to their small sizes and large surface area and hence are proved to be excellent therapeutic agents (Lan et al., 2013). Biomedical applications of gold nanoparticles include tissue or tumor imaging, drug delivery, photo thermal therapy and immunochromatographic identification of pathogens in clinical specimens (Raghavendra, Arunachalam, Annamalai, & Aarrthy, 2014). Gold nanorods have been used in vivo imaging due to the Plasmon resonance absorption and light scattering in the near infrared region (Giljohann et al., 2010).

Colloidal gold have small sizes equal to the biological molecules like DNA and proteins and have been used as efficient drug delivery systems (Amjadi & Farzampour, 2014). Gold nanoparticles can bind with a wide range of organic molecules and can be used as therapeutic agents or vaccine carriers in to the specific cells so that can destroy pathogens. Gold nanoparticles have been used for epidermal delivery of DNA vaccines using gene gun gold method. The walls of the gold nanocages are coated with temperature-sensitive polymer which releases their effectors with interaction of near-infrared irradiations (Amjadi & Farzampour, 2014).

2.5 Saponins

Saponins are triterpenes and steroids present in the roots, tubers, leaves, flowers or seeds of higher plants. The oligosaccharides in their structures are attached to hydroxyl groups through an acetal linkage (Sparg, Light, & Van Staden, 2004). Saponins have been found to be effective in combating tumor and cancer. They arrest the cell cycle and induce apoptosis with IC50 (inhibit cellular proliferation by 50%) values up to 0.2 mM (Vincken et al., 2007).

There are approximately 100 plant families which are reported to contain saponins. Among natural saponins about 150 have significant anticancer properties. The steroidal saponins are mainly found in Agavaceae, Dioscoreaceae, Liliaceae, Solanaceae, Scrophulariaceae, Amaryllidaceae, Leguminosae and Rhamnaceae*;* while triterpene saponins are predominantly present in Acanthopanax, Leguminosae, Araliaceae, Scrophulariaceae, Campanulaceae and Caryophyllaceae. There are more than 11 mainly distinguished classes of saponins including dammaranes, tirucallanes, lupanes, hopanes, oleananes, taraxasteranes, ursanes, cycloartanes, lanostanes, cucurbitanes, and steroidals. Among these saponins, cycloartanes, dammaranes, oleananes, lupanes and steroids showed strong antitumor effect on kinds of cancers (Man, Gao, Zhang, Huang, & Liu, 2010).

Saponins occur not only in plants but also in a few marine animals. The name saponin refers to their soapy nature as they form foams in aqueous solutions. Their demerits include hemolysis of red blood cells, toxicity via the intravenous administration route, deadly effects on fish and snails (Böttger & Melzig, 2013) and inhibition of the growth of moulds. The presence of saponins in the shoots and bark of trees strengthens the point that they help protect the plant from insect attack (Gadelha et al., 2015). Majority of saponins interact with 3-P-hydroxysteroids and form large micelles with bile acids and cholesterol. Saponins are a component of many food plants (Bora, 2014).

Saponins are exploited in a number of traditional and industrial applications owing to their diverse physicochemical and biological properties (Gengatharan, Dykes, & Choo, 2015). As a component of food saponins have been considered as “antinutritional agents” probably due to their bitter taste and have been removed to facilitate human consumption (Bora, 2014).

However, they have been added to food and non-food sources owing to increasing evidence of their health benefits such as cholesterol lowering and anticancer properties in the recent years (Gengatharan et al., 2015; Oleszek & Marston, 2013).

2.5.1 Structure of Saponins

Saponins have a glycosidic and a steroid part. The gylosidic part contains one or more sugar chains and the triterpene/steroid part is called a sapogenin. Saponins are labeled as mono, di-, or tridesmosidic depending upon the number of sugar chains present in their structure.

The sugar chains are attached specific positions such as a single sugar chain is present at C-3 in monodesmosidic saponins. Bidesmosidic saponins have two sugar chains, one attached via an ether linkage at C-3 and one attached through an ester linkage at C-28 (triterpene saponins) or an ether linkage at C-26 (furastanol saponins). The common monosaccharides include: D-glucose (Glc), D-galactose (Gal), D-glucuronic acid (GlcA), D-galacturonic acid (GalA), L-rhamnose (Rha), L-arabinose (Ara), D-xylose (Xyl), and D-fucose (Fuc). The nature of the aglycone and the functional groups attached to it and the number and nature of the sugars adds diversity to this class of compounds (Golemanov, Tcholakova, Denkov, Pelan, & Stoyanov, 2014).

2.5.2 Physicochemical Properties of Saponins

Saponins have an amphiphilic nature due to the presence of a lipid-soluble aglycone and water soluble sugar chain(s) in their structure. They are surface active compounds with detergent, wetting, emulsifying, and foaming properties (Güçlü-Üstündağ & Mazza, 2007). The formation of micelles above a critical concentration in aqueous solutions is termed as critical micelle concentration (cmc). The micelles forming saponins include soybean saponins, saponins from *Saponaria officinalis*, and *Quillaja saponaria* (Argentieri et al., 2008). Solubility enhancement poses a repercussion in the processing of saponins. Monodesmosides can be extracted owing to their poor water solubility in comparison to high solubilizing effect of the co-occurring compounds (Ozturk & McClements, 2016).

The properties of the solvent such as composition and pH play a vital role in the solubility of saponins. In addition to water and alcohols the solubility of saponins in ether, chloroform, benzene, ethyl acetate, or glacial acetic acid has also been reported (Lorent, Quetin-Leclercq, & Mingeot-Leclercq, 2014). Although most of the saponins are bitter in taste the occurrence of sweet saponins has also been reported e.g., the presence of glycyrrhizin acid makes licorice 50 times sweeter than sugar (Ribeiro, Alviano, Barreto, & Coelho, 2013).

Storage or processing induces chemical transformations in the structure of saponins thus modifying their properties. The components of saponins including aglycones, prosapogenins and sugar residues are released by the cleavage of glycosidic and interglycosidic bonds by the process of hydrothermolysis or enzymatic/microbial activity (Lorent et al., 2014). The saponin backbone 'aglycone' has a lipophilic nature and therefore has a different solubility response than the saponin (Lorent et al., 2014).

The physicochemical and biological properties of saponins can be modified by the interaction of sterols, minerals and proteins with them (Ribeiro et al., 2013). The interaction of the saponins with proteins results in the modification the of protein properties such as heat and enzyme stability and surface properties (Thakur et al., 2014).

2.5.3 Biological Properties of Saponins

Among the biological properties of the saponins, hemolysis has been investigated the most. Saponins release the haemoglobin by rupturing erythrocytes. Regardless of the structural similarity variations still exist between members of this diverse group (Ribeiro et al., 2013). The toxicity of saponins to insects, parasites, molluscs and fish and their antifungal, antiviral, and antibacterial activity have been reported. Toxicity of saponins to warm blooded animals is dependent on the method of administration, source, composition, and concentration of the saponin mixture (Lorent et al., 2014).

Saponins have been used in the medical treatment of cancer and many of these compounds are now being in clinical practice. Saponins are preferred for the treatment of cancer and tumor as they kill the tumor/cancerous cells by inducing apoptosis which is helpful in lowering side effects in patients by avoiding necrosis.

The combination of saponins with other anticarcinogenic drugs can yield very efficient treatment regimens against cancer (Waller & Yamasaki, 2013).

2.6 Alcoholic Liver Disease

In the heavy drinkers intracellular accumulation of lipids occurs which causes fatty liver thus leading to benign liver cancer. However, it has been reported recently that steatosis causes progression of hepatic injury as steatosis is frequently found in the liver biopsies of a number of chronic liver diseases (Powell, Jonsson, & Clouston, 2005). The accumulation of fats has been proposed to be due to the impairment of mitochondrial lipid oxidation (Pessayre & Fromenty, 2005). The chronic induction of ethanol with endotoxins is unable to cause alcoholic hepatoxicity (Järveläinen, Fang, Ingelman-Sundberg, & Lindros, 1999), the probable cause of which is mitochondrial remodeling which adapts the liver to alcohol (Han et al., 2012).

The immune system is known to control the inflammatory processes associated with chronic liver diseases (Kita, Van De Water, Gershwin, & Mackay, 2001) as the liver infiltrates have been histologically found to contain both CD8+ and CD4+ T lymphocytes in approx. 40% of ALD patients which are involved in intralobular inflammation, peacemeal necrosis and septal fibrosis (Albano & Vidali, 2010). The lymphocytes isolated from the liver of alcohol consuming rats have been found to have an increased capacity to secrete pro-inflammatory cytokines causing inflammation during the progression of ALD (Batey, Cao, & Gould, 2002). The increasing evidence has indicated that a fatty liver is more prone to factors that lead to inflammation and fibrosis (Day & James, 1998).

2.7 Infection Related Liver Damage

Liver steatosis is also caused by hepatitis C virus (HCV) (Lonardo et al., 2004). An increased progression to fibrosis was found in the patients of high grade steatosis by Adinolfi and his colleagues (Adinolfi et al., 2001), Westin and his colleagues also found that progression of fibrosis was more common in patients with steatosis (Castera et al., 2003; Westin, Nordlinder, Lagging, Norkrans, & Wejstål, 2002).

Both chronic HCV and obesity-related fatty liver disease have almost the same risk factors which include increased BMI (Body Mass Index), type 2 diabetes, increasing age, and alcohol intake—all of which increase the chances of steatosis (Lonardo et al., 2004).

Steatosis also leads to the development of cirrhosis in HCV patients (Wyatt, Baker, Prasad, Gong, & Millson, 2004). The reduction in steatosis probably causes cirrhosis which can be associated with portal-systemic shunting which results in decreased hepatic exposure to insulin (Caldwell & Crespo, 2004). In the case of HCV the viral proteins interfere with mitochondrial function and damage the fatty acid oxidation (Moriya et al., 1998). It has been reported that the prevalence of steatosis is higher in obese patients than lean subjects regardless of viral genotype and resistance to insulin is considered to be a key pathophysiological mechanism (Powell et al., 2005).

The reduction in steatosis upon weight reduction further supports the notion that viral factors are not the only reason of fat accumulation (Hickman et al., 2002). In the case of nonalcoholic steatohepatitis, hepatocyte ballooning occurs thus representing oxidative stress (Zatloukal et al., 2004). The apoptotic hepatocytes were observed in the liver sections of chronic HCV patients with moderate or severe steatosis (Walsh et al., 2004).

2.8 UV Spectroscopy

2.8.1 Color Variation

In the ultraviolet-visible spectroscopy (UV-Vis) the absorption of light by the molecules occurs in ultraviolet-visible region which corresponds to the color of the solutions involved i.e., when the solution color changes from wine red to purple or gray the absorption spectrum broadens and red shifts indicating that the hue of the color and its intensity depended on the stoichiometric ratio in which saponins and the gold solution had been mixed.

It has been reported that the unaggregated gold nanoparticles give wine red colored solution whereas the aggregated AuNps give blue/purple color which progresses to a clear solution with black precipitates e.g., dried nanoparticles are aggregated and cannot be re-dispersed as individual particles.

It was obvious from the color of the AuNps solution that best particles are formed using higher concentrations such as 2mM and at lower molar ratios such as 2:1 and 6:1 as the characteristic LSPR (localized SPR) band for the intense red colored solution appeared in the visible region with peak wavelength around 530nm.

The biopolymers adsorbed on the individual particles affect the solution color and absorbance. The solution color reflects the distance between the adjacent particles e.g., when the particles move closer to each other to distances smaller than 0.1 of their diameter the red color of the solution changes to purple or gray and the absorption spectrum broadens and the red shifts. Colloidal gold solution with particle size ranging from 5 to 60nm is stable for long duration in the absence of any stabilizing agent.

2.8.2 Effect of Ratios and Concentration on UV spectra

The characteristic LSPR band of the AuNps is determined by their size and shape. The absorbance peak increases with the increase in size but it shifts to the far red region in the case of change in shape of the Nps e.g, for colloidal or uneven shaped particles having diameter identical to the spherical AuNps. The absorbance is also termed as optical density of particles and it correlates to the concentration of the AuNp solution. Higher concentrations reduce foaming in the SapAuNp solution. The concentration of the solutions can be measured by their absorbance. In other words both the concentration and absorbance can be calculated by UV-Vis spectroscopy.

CHAPTER 3: MATERIALS AND METHODS

3.1 Materials

Corchorus depressus plant (local name "*Bahu Phali*"), buffer tablets PBS, dissection kits, insulin injections (1ml) and double distilled water (18MΩ resistivity) were used in the study. Gold trichloride acid, tri-hydrate yellow H ($AuCl_4$).$3H_2O$ was purchased from E Merck, D-6100 Darmstadt. Petroleum ether, hydrochloric acid, sulfuric acid, methanol and ethanol were purchased from BDH Laboratory Supplies Poole, BH151TD England.

3.2 Scientific Equipment and Lab Apparatus

UV- Vis spectrum was recorded on double beam UV 2800 spectrophotometer from 350-800nm at a resolution of 1nm. The de-ionized water was used as a reference for UV analysis. The UV was recorded from time to time till 4days to test the stability of AuNps with time. HERMLE (HERMLE Labortechnik GmbH, Siemensstrasse 25, 78564 Wehingen) table top centrifuge Z 326 K was used for removing the impurities from the crude plant extract at 8000 rev for 15mins at 25˚C and for washing the AuNps prior to SEM at 13,000 rev for 15 mins at 25˚C, the resulting pellets were washed thrice with de-ionized water to remove the unreacted constituents and were then re-dispersed in de-ionized water.

The AuNp solutions were sonicated for 2hrs. A thin film of the sample was prepared by droping a small amount of the sample on the grid, blotting paper was used to remove the extra solution and the film on the SEM grid was dried under a mercury lamp for 5 mins. The SEM images were recorded using JEOL-6490A-JSM SEM at a high resolution of 0.5µm-1µm and magnified upto X50, 000 at a voltage of 20kV. SEM images not only depicted the morphology but also aided in the measurement of particle size distribution.

The functional biomolecules involved in the reduction, stabilization and capping of the AuNps were identified by FTIR (Fourier transform infrared spectroscopy) performed on Model Perkin Elmer spectrometer FTIR spectrum 100.

The samples were loaded dropwise on potassium bromide (KBr) pellets and the spectra were recorded at a diffuse mode with 4 cm^{-1} resolution in the mid-IR region between 4000 and 400 $cm^{-1.}$

3.2.1 Aqua Regia

All the lab glassware was washed with freshly prepared aqua regia. Aqua Regia was prepared by mixing HCL and HNO_3 in a 3:1 ratio (3parts HCL: 1 part HNO3, v/v). All the lab glassware required for the synthesis of gold nanoparticles was washed with aqua regia and then rinsed thoroughly with water and dried in oven (40˚C) to avoid unnecessary nucleation during the synthesis and aggregation of gold nanoparticles afterwards.

3.3 Extraction and Purification of Saponins

The plant was thoroughly washed with water. It was shade dried for 3 days and then was ground to fine powder in the grinder. The powder was then added to methanol in 500ml conical flasks (10g/100ml) which were incubated in shaker (Wisd WiseBath) at 120rpm and 37˚C for 2consective days. The plant broth was centrifuged and filtered after shaking using filter paper (Whatman Schleicher & Schuell, Cat.No. 100 125), methanol was evaporated (45˚C) using rotary apparatus (Rotary Evaporator model: Laborota-4000 Germany) and the dried powder containing crude saponins was scratched.

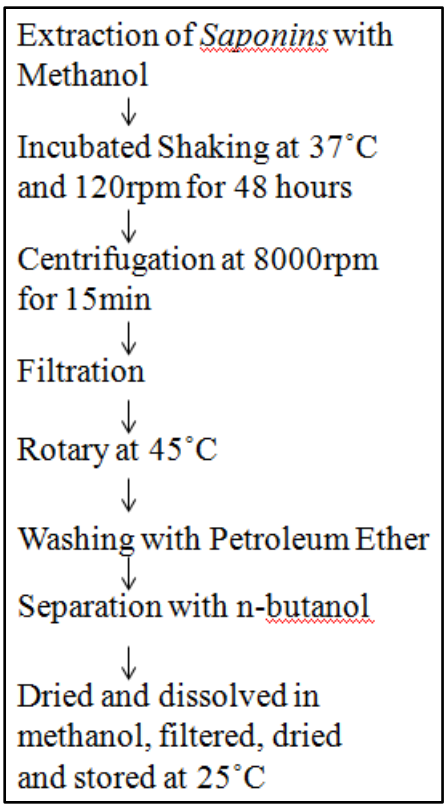

Figure 3.1: Extraction of saponins from the stem of '*Corchorus Depressus'* plant

The powder was washed with petroleum ether to remove lipophilic substances (defatting step in the figure 3.1); the process was repeated till the supernantant was clear. The saponins were finely extracted by dissolving them in water saturated with n-butanol in the separating funnel.

The butanol layer was pipette and saponins were extracted by evaporation. The saponins were further purified by washing with methanol and filtration. The dried powder was scratched and stored in aluminium covered glass vials at room temperature. Reportedly, Saponins are powder at room temperature. They are hygroscopic in nature, are not autoclavable and are stable for atleast a year at room temperature.

3.3.1 Confirmatory test for saponins

The extraction of saponins was confirmed through TLC (Thin Liquid Chromatography). A 5µl drop of saponin solution was loaded on the TLC plate which was immersed in a solvent mixture of chloroform, water and methanol in the ratio 3:2:1 in a beaker which was covered to saturate the inner atmosphere with solvent vapors.

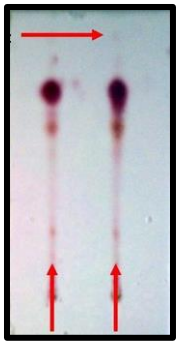

Figure 3.2: Purple bands on the TLC plate confirm the presence of saponins

A filter paper was soaked in the solvent mixture to prevent solvent evaporation. The TLC plate was removed from the beaker after 20 mins, was air dried and sprayed with 10%H_2SO_4 and placed in oven for 15mins at 115˚C. Purple bands confirmed the presence of saponins.

3.4 Synthesis of Saponin Gold Nanoparticles (SapAuNps)

The synthesis of AuNps requires a precursor, stabilizer and a reducing agent, gold salt serves as the precursor. In the green synthesis of AuNps the plant extract acts both as a stabilizer and a reducing agent. There are two main mechanisms of synthesizing AuNps namely; Turkevich synthesis and Brust and Schriffin synthesis. Turkevich synthesis is a one phase mechanism involving a polar solvent and a single reducing and stabilizing agent. On the other hand Brust and schriffin synthesis is two phase synthesis mechanism in which there is a phase transfer catalyst and reducing and stabilizing agents are not alike.

3.4.1 Study Design

The synthesis strategy of Turkevich and Frens (Zabetakis et al., 2012) was employed in the study to check its significance in the case of green synthesis.

Table 3.1: Calculation of concentrations and ratios for AuNps synthesis

Concentration of Gold Solutions	Ratios(Sap/Au) mixed in multiples of five
A=0.3mM	1=2:1(10:5)
B=0.6mM	2=6:1(30:5)
C=0.8mM	3=10:1(50:5)
D=1mM	4=14:1(70:5)
E=2mM	5=20:1(100:5)

The five different concentrations of gold solutions labeled as A=0.3mM,B=0.6mM.C=0.8mM,D=1mM,E=2mM, were tested against five different ratios with saponins 2:1,6:1,10:1,14:1 and 20:1 designated as 1,2,3,4,5 respectively.

The choice of the concentrations and ratios is based on the inference from the model of Kara and William (Zabetakis et al., 2012). The ratio of saponin to gold was kept larger and the gold ratio was kept constant in reference to the Turkevich, Frens and Kumar models. The gold solutions were stored in aluminium covered reagent bottles (100ml) to minimize photoinduced oxidation. Stock solution of saponins was prepared in DDW (1mg/ml), the solution of saponins is reported to be stable for one month at 2-8˚C.

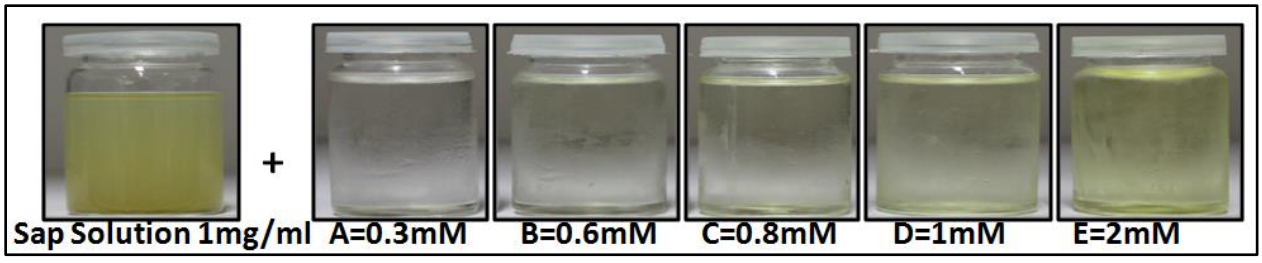

Figure 3.3: Saponin solution and gold solutions of different concentrations

All the solutions were refrigerated at 4˚C. The gold and saponin solutions were mixed in different ratios in multiples of five. The ratios set in multiples other than five e.g., multiples of 2 or 3 gave poor results. Moreover, methanol is not a preferred solvent for saponins as it gets evaporated by continuous stirring for 1-2 hrs.

Saponins formed foams in mixtures which disappeared by increasing gold salt concentration. Heating is avoided as high temperature is reported to increase the diameter of the particles due to the formation of hollow nanoparticles.

Initially 5ml of each gold concentration was added to the 100ml conical flask which was set on stirring on a stirrer. The stirring was continued until vortex was reached, then the saponin solution was added upon reflux according to the selected Sap/Au ratios. A change in the color of the mixture was observed in the case of bioreduction of gold which indicated nanoparticle formation. The color began to appear after 10 mins of stirring and changed from yellow to pink to orange red to wine red after 20 mins.

A yellow to purple/brown color transition was observed with some concentrations which indicated poor AuNps. The change in color indicates the reduction of chloroauric ions by saponins which results in the formation of gold nanoparticles. The reaction was stopped after 20 mins and UV analysis was performed.

3.5 Animal Study

So far the experimental models of full progression of ALD have not been successfully established however a number of animal studies have aided in understanding the underlying mechanisms of the various stages of ALD (Arteel, 2011) (Brandon-Warner, Schrum, Schmidt, & McKillop, 2012). It has been shown that the acute administration of ethanol significantly affects the hepatic mitochondrial function, oxidative stress, and inflammatory responses. It has been shown experimentally that acute ethanol binge causes autophagy in the liver (Ding et al., 2010).

3.5.1 Animals

The study was conducted on eight weeks old (50) female *Balb-c* mice strain purchased from NIH (National Institute of Health) located in Chakk Shehzaad in Islamabad, Pakistan. Mice were kept in cages in the laboratory animal house of the institution, NUST (National University of Sciences and Technology).

The research work was conducted after the approval of project from IRB (SMME, NUST) and all the laboratory guidelines concerning the animals were followed.

3.5.2 Histopathology

The tissues were collected immediately after anesthesia to avoid postmortem autolysis and decomposition. A stock solution of 200ml of 10% formalin was prepared by adding 20ml of 40% formaldehyde to 180ml of distilled water in 1:9 and was buffered with PBS (phosphate buffered saline) to neutralize the acidic effect of formalin as the unbuffered formalin is acidic (3-4pH) and can react with hemoglobin in the tissues to produce dark brown acid formaldehyde haematin precipitates which can complicate the histological interpretation.

The tissues were stored in formalin at room temperature as freezing causes ice crystal formation which alters tissue morphology. The organs were sliced into 5mm pieces so that formalin can easily penetrate the tissue to avoid dryness which is reported to create artifacts in histological examination. The tissues were stained with hematoxylin and eosin staining for histopathological examination. The histopathological reports of the liver, spleen and kidney biopsies refer to Islamabad Diagnostic centre, Kohistan road, F-8 Markaz, Islamabad.

3.5.3 Induction Protocol

The doze was set in accordance with the cirrhosis model of Marco and Paolo (Domenicali et al., 2009) however, owing to the difference in mice strains the doze was first optimized.

3.5.3.1 Optimization

The mice were divided into three groups namely: G-1, G-2 and G-3. The first group was given 40µl, 2µl/g body weight, doze (CCl_4 in paraffin oil (50%v/v) twice weekly (Monday and Friday). The second and third groups were given 30µl and 20µl of the same doze respectively for 2 weeks. In contrast to the model of Marco and Poalo (Domenicali et al., 2009) 40µl doze was lethal to Balb/c mice and the mice could not survive the second week. The 2nd group of mice survived the first week in a better condition but their condition became worse in the 2nd week as they became extremely weak and lost weight.

The 3rd group of mice, given 20µl doze, survived the first and the second week in a condition better than the first two groups therefore 20µl doze was set as the optimized doze to induce liver inflammation in Balb/c mice.

3.5.3.2 Doze Setting

A 20ml fresh stock solution of CCL_4 in Paraffin oil (50%v/v) was prepared after every four weeks. The 20µl doze containing 1µl/g of CCl_4 and Paraffin oil(50%v/v) each was administered intraperitonealy twice weekly (Monday and Friday) for 13 weeks. In addition to I.p. administration, 5% ethanol was also given thrice weekly (Tuesday, Wednesday and Thursday) in drinking water to enhance hepatotoxicity.

3.5.3.3 Inflammation Model

The liver toxicity model of inflammation lapsing a time of 13 weeks was prepared by the intraperitoneal (I.p.) induction of CCl_4 in mice. Initially the mice were divided into 10 groups comprising 5 mice each. The mice were acclimatized for a week on tap water and pelleted mouse diet before induction with CCl_4.

3.5.4 Treatment

The mice were given intravenous treatment with saponins and their AuNps for seven weeks. After the successful induction of inflammation in the liver, three groups of mice were selected for the treatment. The anti-inflammatory activity of saponins has already been reported so the aim of the study was to test the significance of SapAuNps to treat inflammation.

3.5.4.1 Treatment Plan

The diseased mice were divided into three groups. One of the groups was left untreated while the other two were given treatment. A comparison of doze effectiveness was drawn between the two treated groups. The treatment was given via the intravenous (i.v.) route, as AuNPs are reported to be toxic when given orally. The intravenous route of administration was preferred for treatment because large amount of AuNPs are taken up by the liver and spleen via systemic administration. Mice were given i.v. injections thrice weekly (Monday, Wednesday and Friday) containing 0.04mlof doze per 1ml of blood or 4ml/kg body weight for seven weeks.

CHAPTER 4: RESULTS

4.1 Balb/c Model of Liver Inflammation

The liver disease progresses slowly in different stages. After 6 weeks of CCl_4 induction micro vesicular steatosis was reported which was followed by mild inflammation in the 9th week and advanced/moderate inflammation in the 13th week as shown in the figure 4.1. The mice dissected after 13 weeks had severe inflammation in the liver and spleen. The histopathological reports confirmed inflamed portal tracts and congestion in the liver and infiltration of megakaryotes in the spleen.

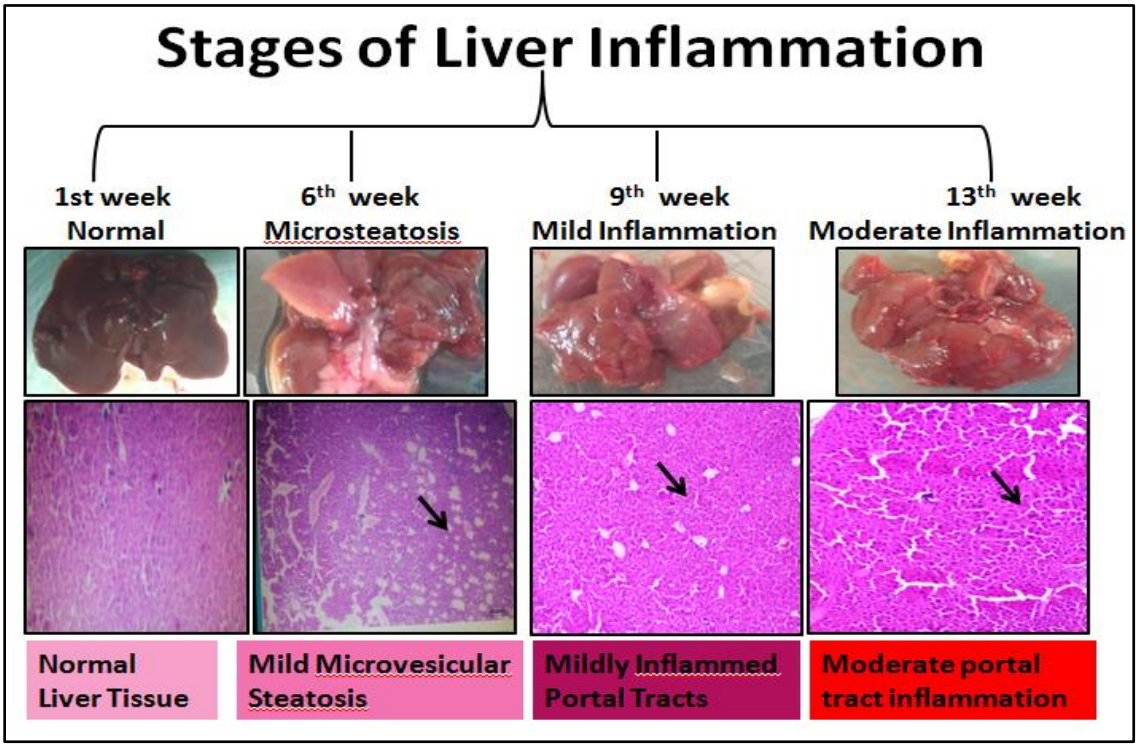

Figure 4.1: Stages of liver inflammation

4.1.1 Effect of CCl_4 Induction on other Organs

The analysis of organs upon dissection clearly revealed that intraperitoneal induction of CCl_4 did not affect the other vital organs including the heart, lungs and kidneys. The induction with CCl_4 and alcohol damaged the liver only.

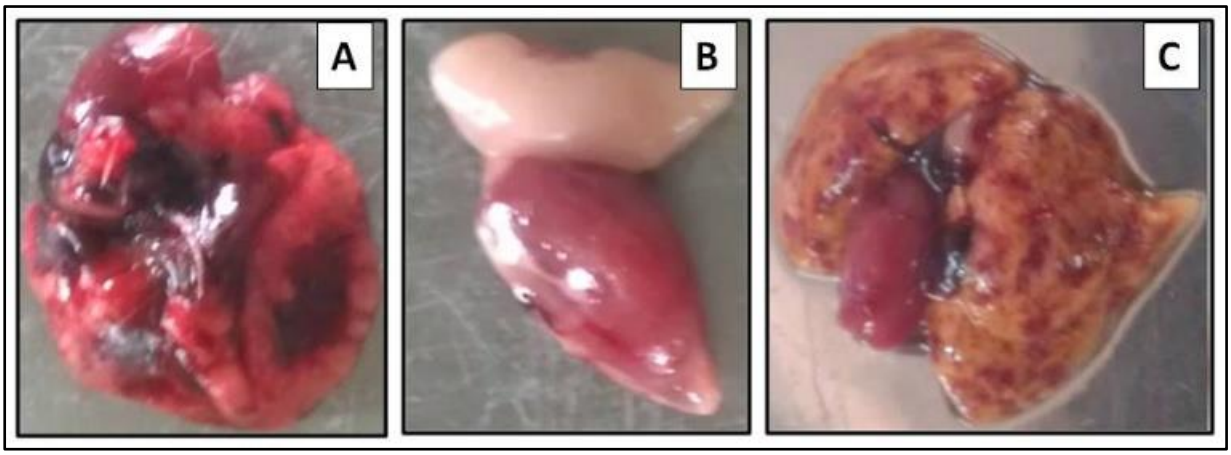

Figure 4.2: Effect of CCl_4 induction on other organs including the heart, lungs and kidneys. (A) Heart of diseased mice. (B) Kidney of diseased mice. (C) Lungs of diseased mice.

4.1.2 Peritoneal Adhesions

Upon dissection, adhesions in the intraperitoneal cavity were found which strongly agree with the experimental model of Marco and Paolo (Domenicali et al., 2009)i.e., paraffin oil given as a delivery agent in 50% v/v along with CCl_4 for inducing liver damage causes adhesions in the abdominal cavity. The intestines and other abdominal organs had severe adhesions upon dissection in the 13^{th} week as evident from the figure 4.3.

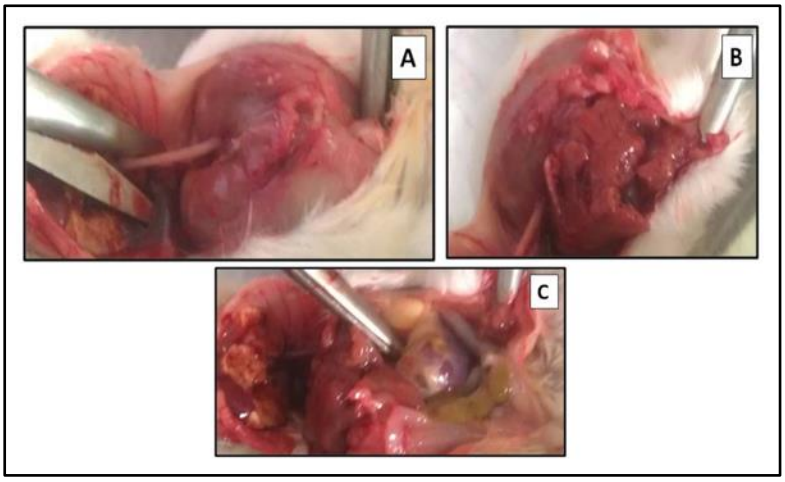

Figure 4.3: Peritoneal adhesions in the abdominal cavity upon CCl_4 and paraffin induction (50%v/v). (A), (B) & (C) Peritoneal adhesions in the intraperitoneal cavity of diseased mice.

4.1.3 Statistical Analysis of Effect of CCl_4 Induction

The line and column plots for body and organ weights were plotted in Microsoft Excel. The customized error bars were applied on the plots using standard deviation. A p value less than 0.05 was considered to be statistically significant. ANOVA (One-Way Analysis of Variance) was performed for evaluating the treated and non-treated mice groups.

4.1.3.1 Effect of CCl_4 Induction on Body Weights

In the first four weeks the differences in the mean values between the normal and diseased groups are greater (4.65) than would be expected by chance; there is a statistically significant difference ($p = <0.001$). The t-value is 7.59. The marked reduction in body weights is probably due to excessive alcohol consumption. The mice consumed too much alcohol in the first four weeks and did not consume enough mouse diet which made them weak. The mice were mostly found drowsy whenever visited. In the next six weeks the weight of the mice increased, gradually in the 4-6 weeks and sharply in the 7-9 weeks.

The differences in the mean values between the normal and diseased groups are greater (3.45) than would be expected by chance; there is a statistically significant difference ($p = <0.001$). The t-value is 4.49. In the 4-6 weeks, the mice stopped consuming alcohol probably due to pain in the liver as alcohol enhances hepatotoxicity. The body weights of mice increased gradually as the diet improved but increased markedly in the 7^{th}, 8^{th} and 9^{th} weeks indicating inflammation and ascites.

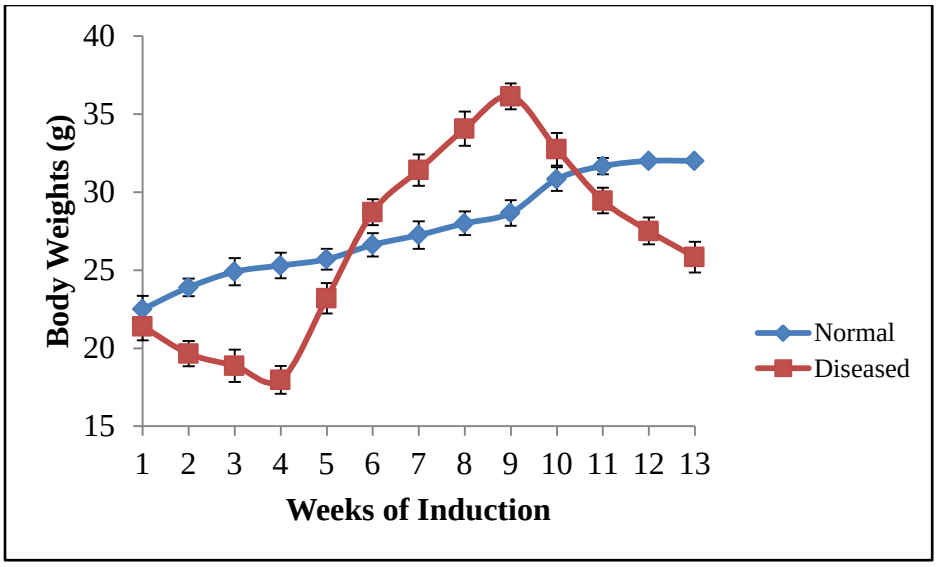

Figure 4.4: Body weights of normal and diseased mice Vs weeks of induction

The body weight of the mice decreased in the last 4 weeks. The differences in the mean values between the normal and diseased groups are greater (2.73) than would be expected by chance hence, there is a statistically significant difference ($p = 0.010$). The t value is 2.787. The weights dropped drastically in the last two weeks indicating a rapid progression towards fibrosis and cirrhosis.

4.1.3.2 Stages of Spleen Damage

The weight of the spleen changed significantly during different stages of liver damage indicating a close relationship between liver and spleen. The changes in the liver affect the spleen in one way or the other. The inflammation in the spleen termed as 'spleenomegally' was observed along with liver inflammation which supports the notion that the factors which adversely affect the liver, affect the spleen as well.

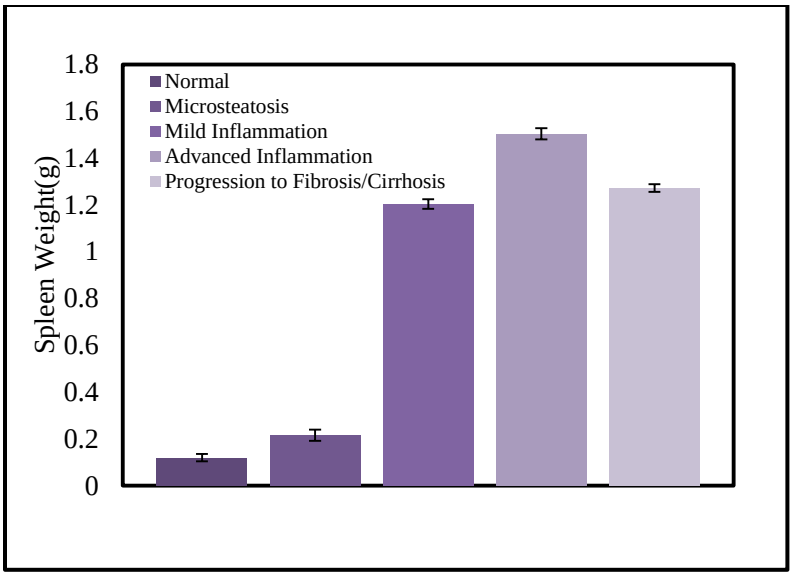

Figure 4.5: Spleen weights of mice during different disease stages

The differences in the mean values of spleen weights at different disease stages are greater than would be expected by chance; there is a statistically significant difference ($p = <0.001$). Pairwise multiple comparisons were carried out between different stages which indicated that the weights of the spleen remained significantly different at all stages ($p<0.001$) reflecting the direct effect of liver damage on the spleen. The weight of the spleen tends to decrease when the disease progresses to fibrosis/cirrhosis indicating the formation of fibers.

4.1.3.3 Splenomegaly

The spleen tends to inflame upon liver damage, it was observed upon dissection that swelling in the spleen occurs as result of liver damage. The inflamed spleen is an indication of liver damage.

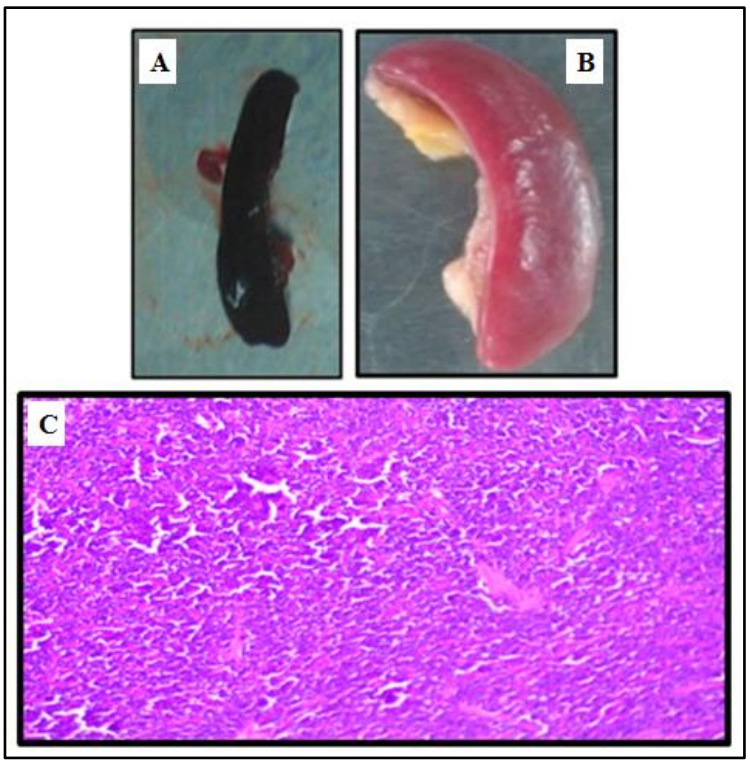

Figure 4.6: (A), (B) Comparison of the normal and inflamed spleen upon dissection in the 11th week of CCl_4 induction. (C) The histopathology of the spleen confirmed moderate inflammation in the 11th week.

4.1.3.4 Stages of Liver Damage

The weight of the liver also reveals significant variations upon disease progression. The administration of CCl_4 over 13 weeks damages the liver in four different stages.

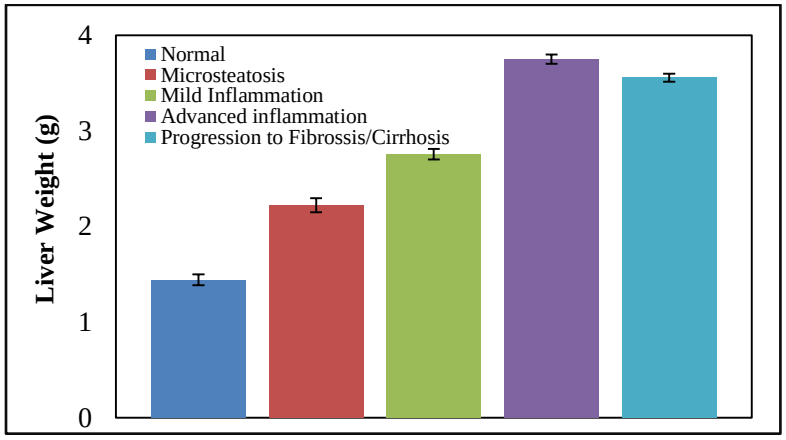

Figure 4.7: Liver weights of mice during different disease stages

The differences in the mean values at different stages of liver damage are greater than would be expected by chance; there is a statistically significant difference ($p = <0.001$). Pairwise multiple comparisons reveal significant difference between all stages ($p<0.001$). The difference of means is the greatest (Diff of means=2.308, t=64.33) between the normal and advanced inflammation stage, indicating significant weight change upon severe liver damage.

As the disease progresses towards fibrosis probably in the 12^{th} and 13^{th} week the weight of the liver decreases a little in comparison to the advanced liver inflammation stage (Diff of means=0.192, t=5.352), however in the rest of the stages i.e., from normal to advanced inflammation stage the weight of the liver increases continuously. A decrease in liver weight after the advanced inflammation indicates progression towards fibrosis/cirrhosis. The fibers probably replace the normal liver tissue, creating structural irregularities which are apparent upon dissection.

4.2 UV-Vis Spectroscopy

The synthesis of gold nanoparticles was initially confirmed by UV spectroscopy. It was proved experimentally that the stoichiometric ratios and concentrations have a significant effect upon the color and UV spectra of AuNps.

4.2.1 Color Variation

In the ultraviolet-visible spectroscopy (UV-Vis) the absorption of light by the molecules occurs in ultraviolet-visible region which corresponds to the color of the solutions involved i.e., when the solution color changes from wine red to purple or gray the absorption spectrum broadens and red shifts indicating that the hue of the color and its intensity depended on the stoichiometric ratio in which saponins and the gold solution had been mixed.

It has been reported that the unaggregated gold nanoparticles give wine red colored solution whereas the aggregated AuNps give blue/purple color which progresses to a clear solution with black precipitates e.g., dried nanoparticles are aggregated and cannot be re-dispersed as individual particles.

It was obvious from the color of the AuNps solution that best particles are formed using higher concentrations such as 2mM and at lower molar ratios such as 2:1 and 6:1 as the characteristic LSPR band for the intense red colored solution appeared in the visible region with peak wavelength around 530nm.

The biopolymers adsorbed on the individual particles affect the solution color and absorbance. The solution color reflects the distance between the adjacent particles e.g., when the particles move closer to each other to distances smaller than 0.1 of their diameter the red color of the solution changes to purple or gray and the absorption spectrum broadens and the red shifts. Colloidal gold solution with particle size ranging from 5 to 60nm is stable for long duration in the absence of any stabilizing agent (Amendola & Meneghetti, 2009).

4.2.2 Effect of Ratios and Concentration on UV spectra

The characteristic LSPR (localized SPR) band of the AuNps is determined by their size and shape. The absorbance peak increases with the increase in size but it shifts to the far red region in the case of change in shape of the Nps e.g, for colloidal or uneven shaped particles having diameter identical to the spherical AuNps.

The absorbance is also termed as optical density of particles and it correlates to the concentration of the AuNp solution (Srivastava, Yadev, Rai, Ganguly, & Deb, 2012). Higher concentrations reduce foaming in the SapAuNp solution. The concentration of the solutions can be measured by their absorbance. In other words both the concentration and absorbance can be calculated by UV-Vis spectroscopy.

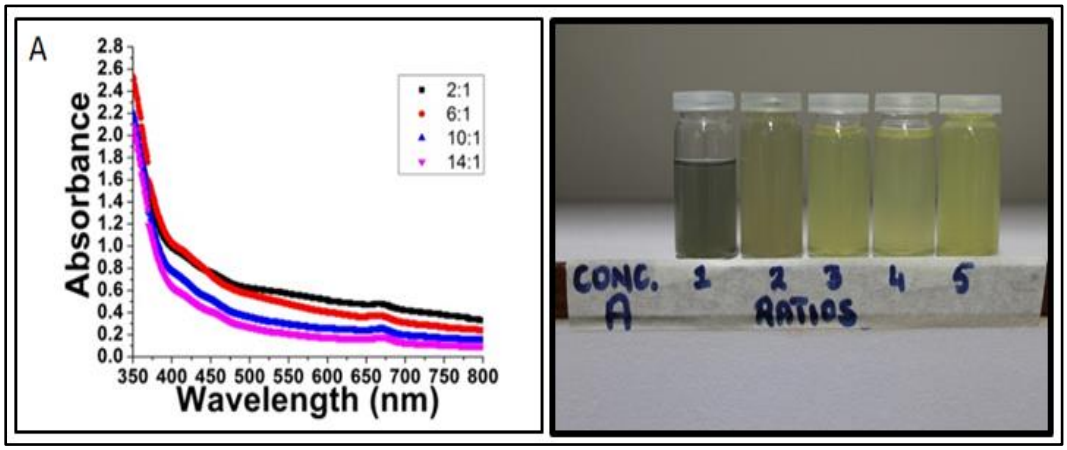

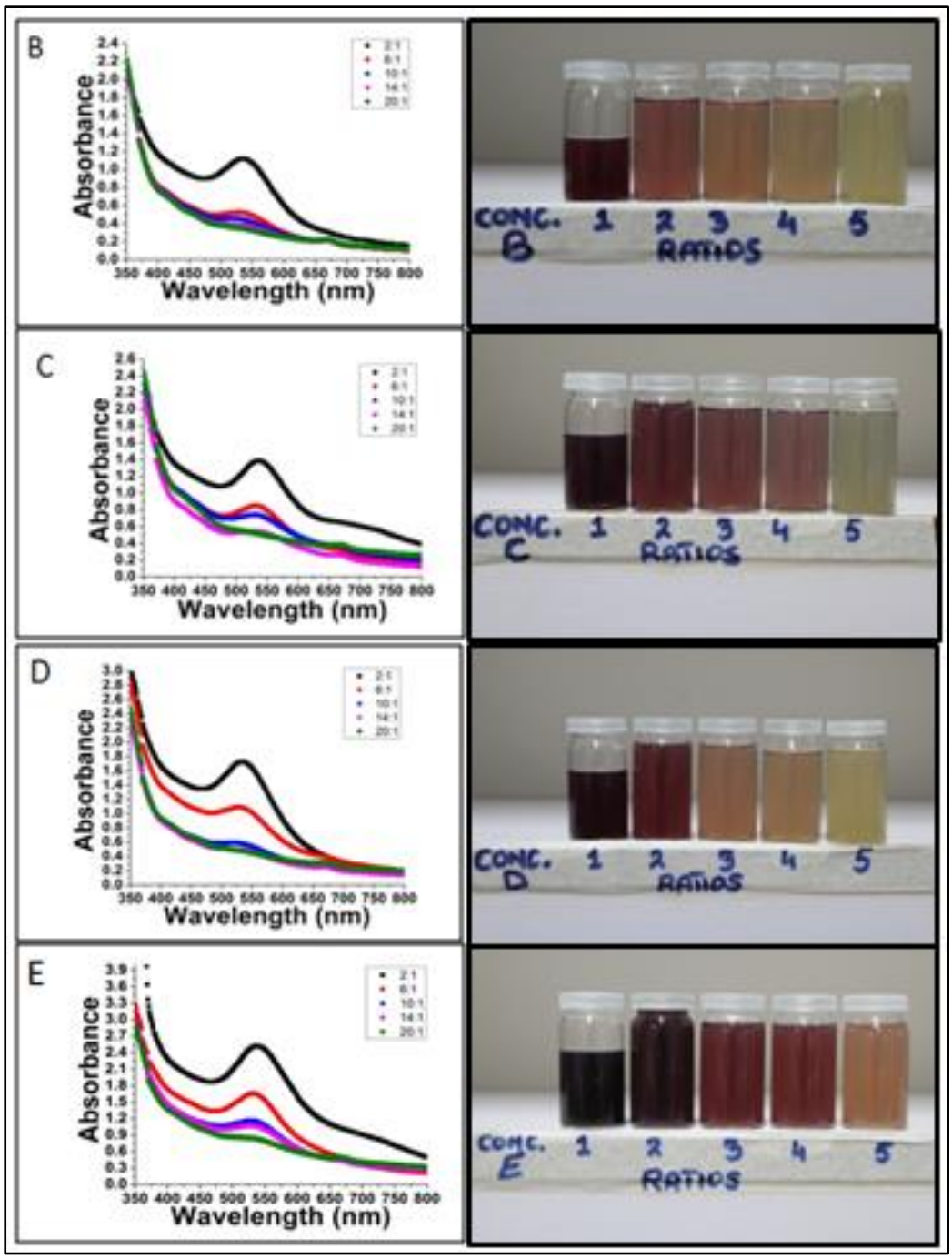

Figure 4.8: The solutions and UV spectra of SapAuNps formed using different ratios and gold salt concentrations. (A), (B), (C), (D) & (E) The UV spectra recorded at various time intervals and colors of solutions which are prepared using 0.3mM, 0.6mM, 0.8mM, 1mM and 2mM gold solution and at Sap/Au ratios 2:1-20:1 keeping the concentration of gold solution constant.

It has been observed that with the increase in gold salt concentration the peak sharpens and becomes closer to 520nm as is obvious from the figure 4.4 the peak of the highest concentration selected is the sharpest and shows maximum absorption. Absorption spectrum reveals the concentration of the AuNps, the greater the concentration the greater the absorption.

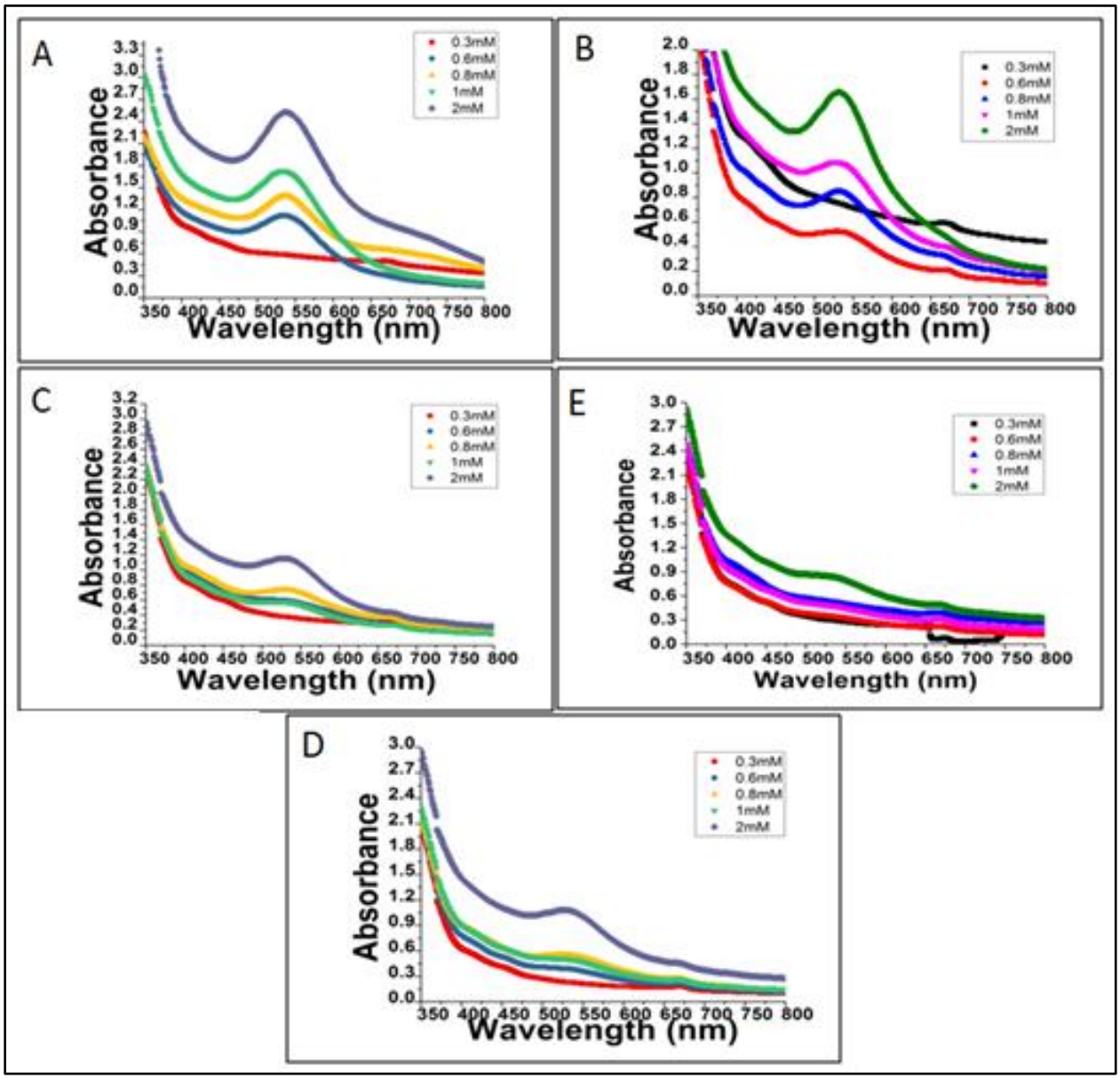

Figure 4.9: Comparison of all concentrations at different ratios (A to E)

In comparison to chemical synthesis as narrated by Turkevich-Frens, Kumar and Kara where lower concentration of gold salt solution below 0.8mM and above 0.3mM i.e., 0.6mM gives smaller and monodispersed particles, green synthesis gives the same size nanoparticles at higher gold salt concentration i.e., 2mM indicating that plant extracts are weak reducing agents. In the chemical synthesis large particles are formed at lower concentrations whereas in green synthesis colloidal particles are formed at lower gold salt concentrations such as 0.3mM and 0.6mM and spherical nanoparticles are formed at concentrations above 0.8mM.

Colloidal and larger AuNps are formed at lower concentrations and spherical, smaller and monodispersed particles are formed at higher concentrations. The large particle size at low concentrations is probably because of low electrolyte concentration which hinders coagulation resulting in increased size of particles.

A significant change is observed in the absorption spectrum with the change in ratios, it's clear from the fig. that all the concentrations generate better peaks at lower ratios i.e., 2:1 and 6:1etc. It appears as if with the increase in ratios the solution becomes saturated with saponins and the gold nanoparticles are submerged.

4.2.3 Stability with Time

It is noteworthy that the SapAuNps take time to stabilize themselves, the fig clearly indicates the stability attained with the passage of time. In most cases, close to 90% of nanoparticle formation was complete by the 6th hour as thereafter the absorbance at different kmax either increased only marginally or remained unchanged for several hours before beginning to decline.

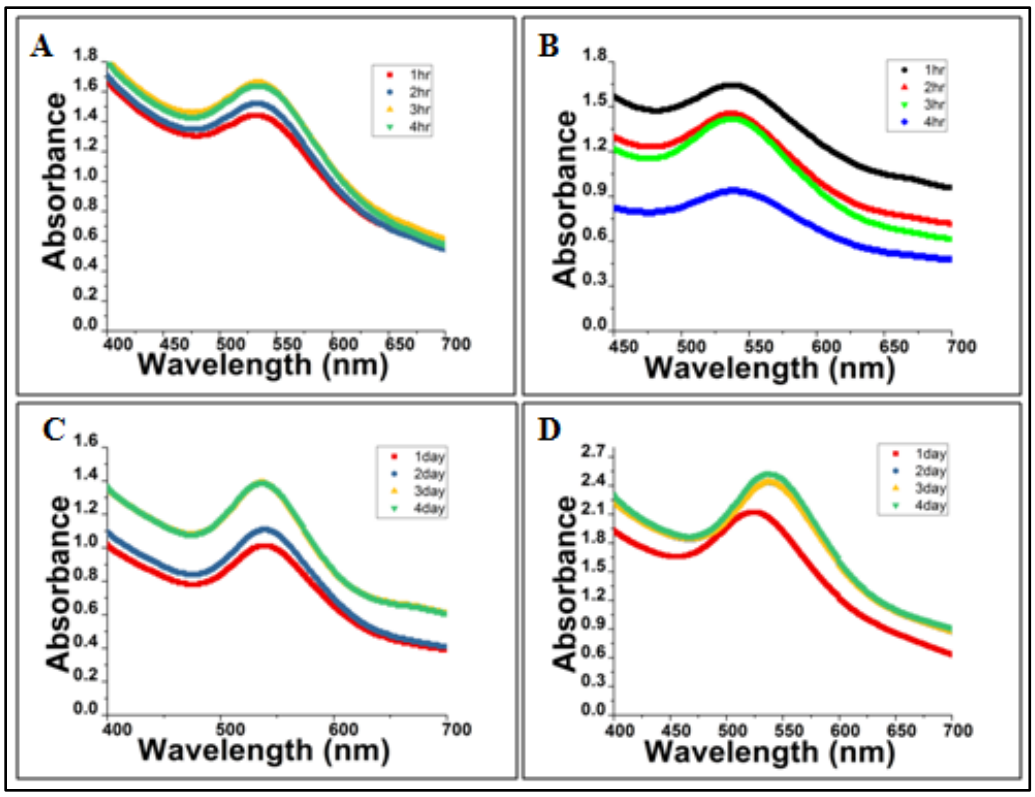

Figure 4.10: The stability analysis of best ratios with time

The decline may be due to the suspended destabilization of the nanoparticles leading to their agglomeration past the colloidal state. In all the spectra, the presence of a single peak in the visible region is attributable to the Transverse Plasmon Resonance (TPR) band, which arises due to the formation of spherical shaped AuNps. This was confirmed by the SEM and TEM micrographs, described below, which revealed the formation of spherical AuNps when these metal: extract combinations were used.

4.3 Scanning Electron Micrograph

The SEM analysis reveals that smaller, spherical and monodispersed AuNps are generated with the higher gold salt concentrations and lower ratios. It is evident from the figure 4.6 that colloidal particles are formed at lower concentrations and lower ratios. With increasing concentrations a decrease in polydispersity and diameter of AuNps is observed.

The reduction of Au^{+3} ions on the surface of AuNps increases the diameter of particles and AuNps larger than 20nm are generated. The increase in diameter is directly related to the amount of the gold reduced. Colloidal gold solution with particle size ranging from 5 to 60nm is stable for long duration in the absence of any stabilizing agent. The change in concentrations and ratios affect the size of SapAuNps. A significant difference in size of the particles is evident from the figure 4.6. As the concentration increases the particle size decreases. The controlled reduction of gold results in the formation of spherical particles because spheres are the lowest-energy shape.

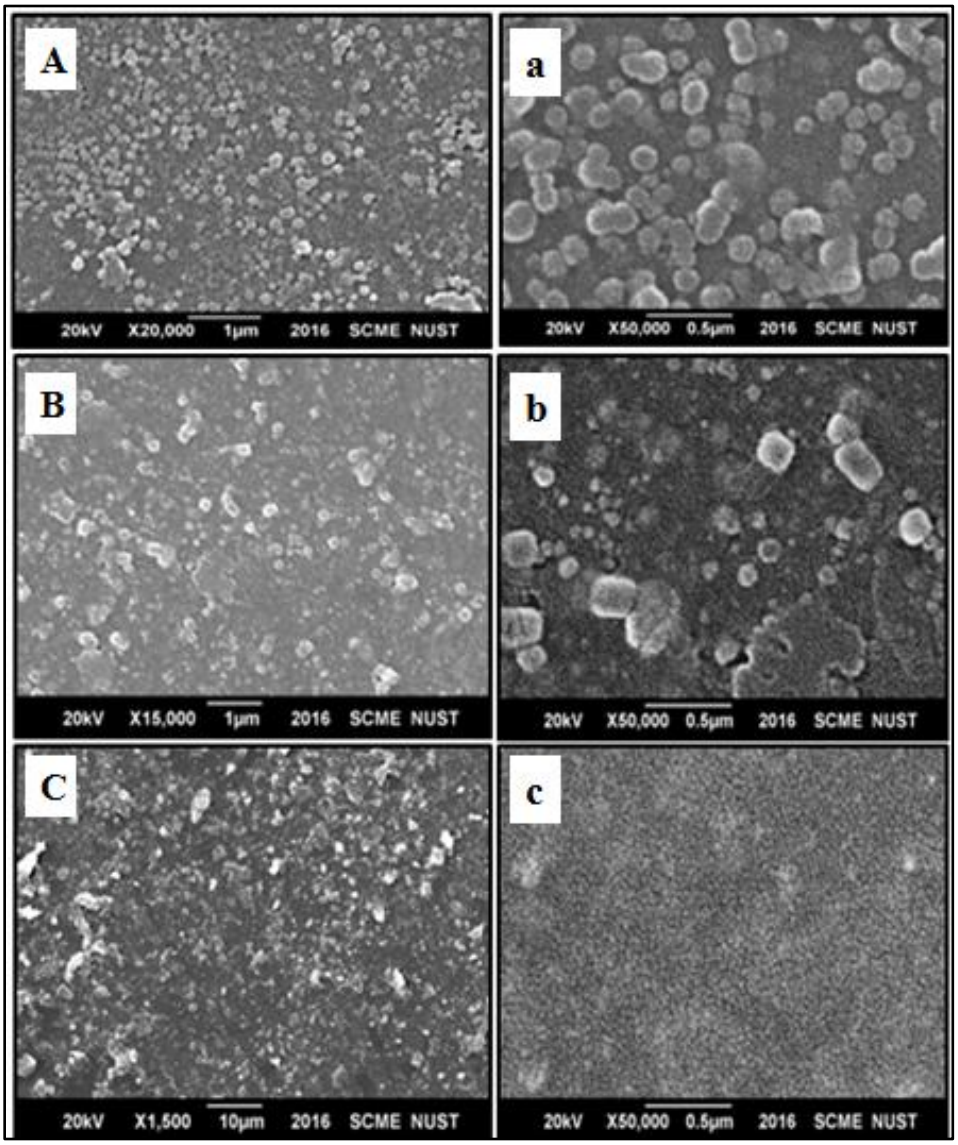

Figure 4.11: Scanning electron micrograph of SapAuNps prepared using 0.6mM gold solution (A, a), 0.8mM gold solution (B, b) and 2mM gold solution (C, c).

4.4 FTIR Spectroscopy

Saponins are classified as steroid glycosides on the basis of their molecular structure. The steroid glycosides contain a sugar moiety attached to the triterpene or steroid aglycone and are termed as monodesmosidic, bidesmosidic and tridesmosidic respectively depending upon the number of sugar chains. The non-sacharide portion of the saponin molecule is an aglycone called genin or sapogenin depending upon which they are categorized into three main classes namely; triterpene glycosides, steroid glycosides and steroid alkaloid glycosides (Hostettmann & Marston, 2005).

Nanoparticles exhibit unique features in comparison to their bulk form owing to their high surface to volume ratio. The FTIR spectrum is a vibrational spectrum of the nanoparticles produced as a result of the oscillations of the atoms present on their surface. It is clear from the figure that the saponin gold nanoparticles (SapAuNps) show significant variations in their vibrational spectra in comparison to the saponin spectrum. In an IR spectrum the width and intensity of peaks depends upon the particle size, with the increase in particle size the width of the peak decreases and intensity increases. The FTIR spectra of the nanoparticles containing some adsorbates show additional peaks in comparison to the FTIR pattern of bare nanoparticles. When the particle size increases from 9 nm to 33 nm, new bands appear with a shift in frequencies (Mohadesi et al., 2016).

The particle size affects the dipolar interactions e.g., when the particle size increases the frequencies of certain bands tend to decrease due to the repulsive dipolar interactions on the other hand when the particle size decreases band broadening occurs perhaps to the presence of cations of the different shells on the same site. Saponins are triterpenoid glycosides and FTIR studies reveal phenolic groups as the potential biomolecules involved in the reduction, capping and stabilization of SapAuNps (Abbasi et al., 2014).

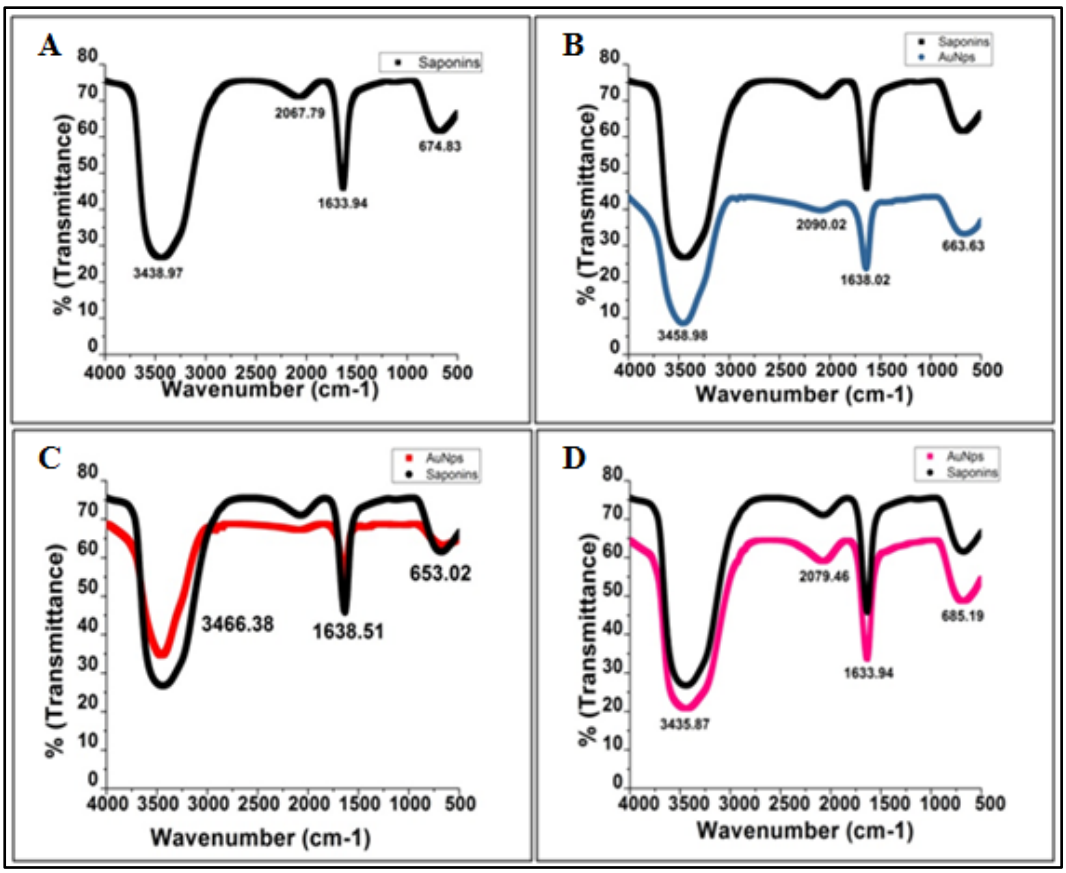

Figure 4.12: (A) FTIR spectra of Saponin. (B) Comparison of the FTIR spectra of Saponins with SapAuNps prepared using 0.6mM gold solution (B), 0.8mM gold solution (C) and 2mM gold solution in the Sap/Au 2:1 ratio.

4.5 Statistical Analysis of Effect of Treatment

The body and organ weights are represented in line and column graphs which are plotted in Microsoft Excel. A p value less than 0.05 is considered to be significant. Customized error bars are applied on the graphs for error analysis.

4.5.1 Effect on body weights w/wo Treatment

The mice were dissected after seven weeks of treatment and variations in the liver condition were observed. Significant variations in the body weights were observed among the three groups (Fig.3).

The mice treated with saponins became extremely weak and lost weight whereas the weight of the non treated mice and the mice treated with SapAuNps increased numerically with or without (w/wo) the treatment. The weight of the organs also revealed significant differences.

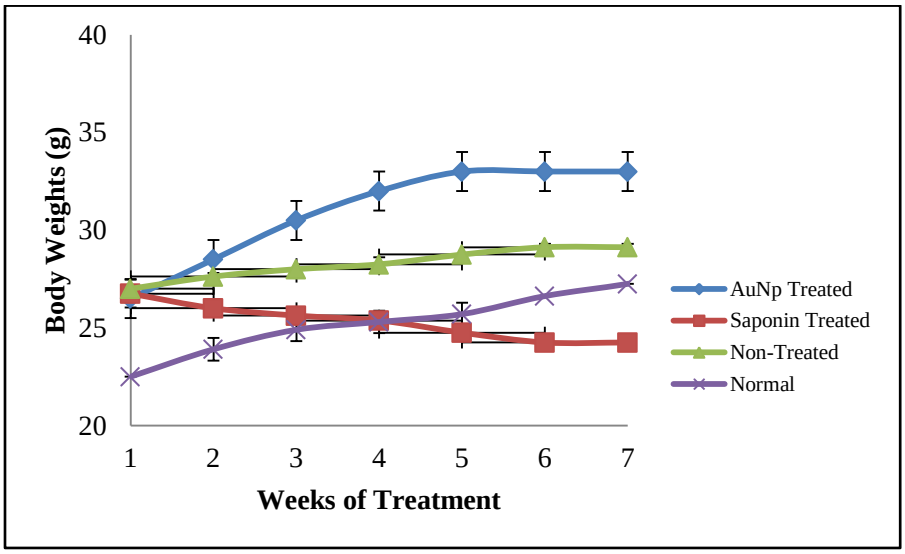

Figure 4.13: Body weights of treated and non-treated mice Vs seven weeks of treatment

Since the differences in the mean body weights among different treatment groups are greater than the differences that are expected by chance so there is a statistically significant difference ($p = <0.001$). Pairwise multiple comparisons revealed significant differences between all the treatment groups except between normal and SapAuNps treated group ($p=0.061$, $t=2.293$) and between non-treated and saponin treated groups ($p=0.059$, $t=2.494$). The graphs clearly indicate that SapAuNps are effective in recovering liver inflammation as the damage regresses back to normal, the weight changes; moreover the saponins have no potential health effect as evident by the decrease in body weight.

The significant weight reduction in the saponin treated mice group is either because of the administration route or because of the hemolytic activity of saponins (Güçlü-Üstündağ & Mazza, 2007). The intravenous route of administration is reported to cause toxicity. Saponins are not only notorious for their hemolytic activity but are also reported to interact with 3-β hydroxysteroids forming large micelles with bile acids and cholesterol (Güçlü-Üstündağ & Mazza, 2007).

4.5.2 Effect on Spleen Weights w/wo treatment

The spleen weights show marked changes upon different treatments. Since the differences in the mean spleen weights among different treatment groups are greater than the differences expected by chance hence, there is a statistically significant difference (p = <0.001). Pairwise multiple comparisons revealed significant differences between all treatment groups.

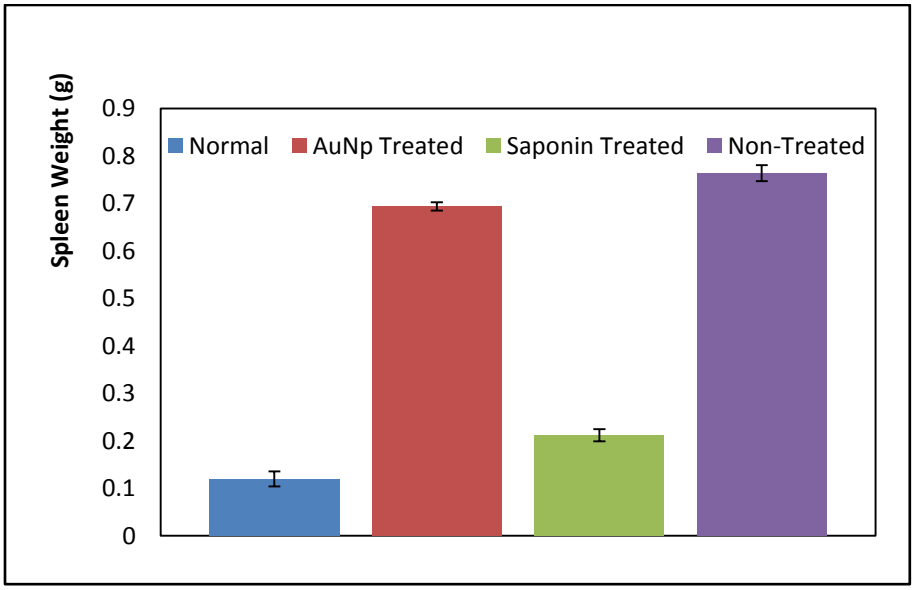

Figure 4.14: Spleen weights of treated and non-treated mice

4.5.3 Effect on Liver Weights w/wo Treatment

The differences in the means of the liver weights among the treatment groups are greater than the difference expected by chance so it is a statistically significant difference (p = <0.001).

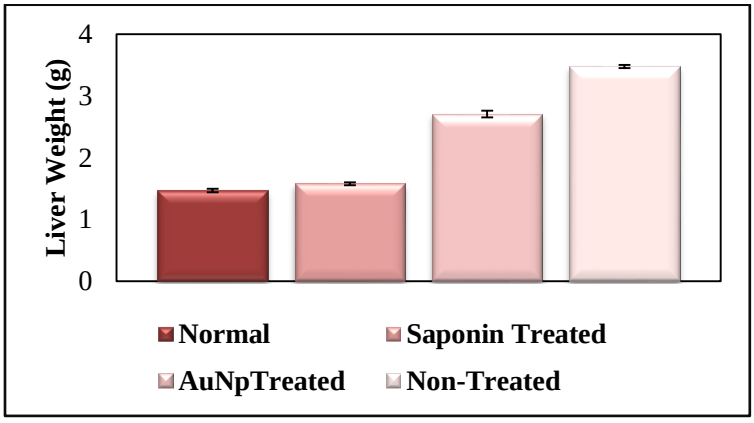

Figure 4.15: Liver weights of treated and non-treated mice

CHAPTER 5: DISCUSSION

5.1 Recovery of the Liver w/wo Treatment

The liver weights of all the three mice groups were nearly the same i.e., no significant variation in liver weights was observed upon dissection; however the histopathologies revealed marked differences among the three. The non-treated mice and the mice treated with saponins had almost the same histopathological results (Figure 5.1).

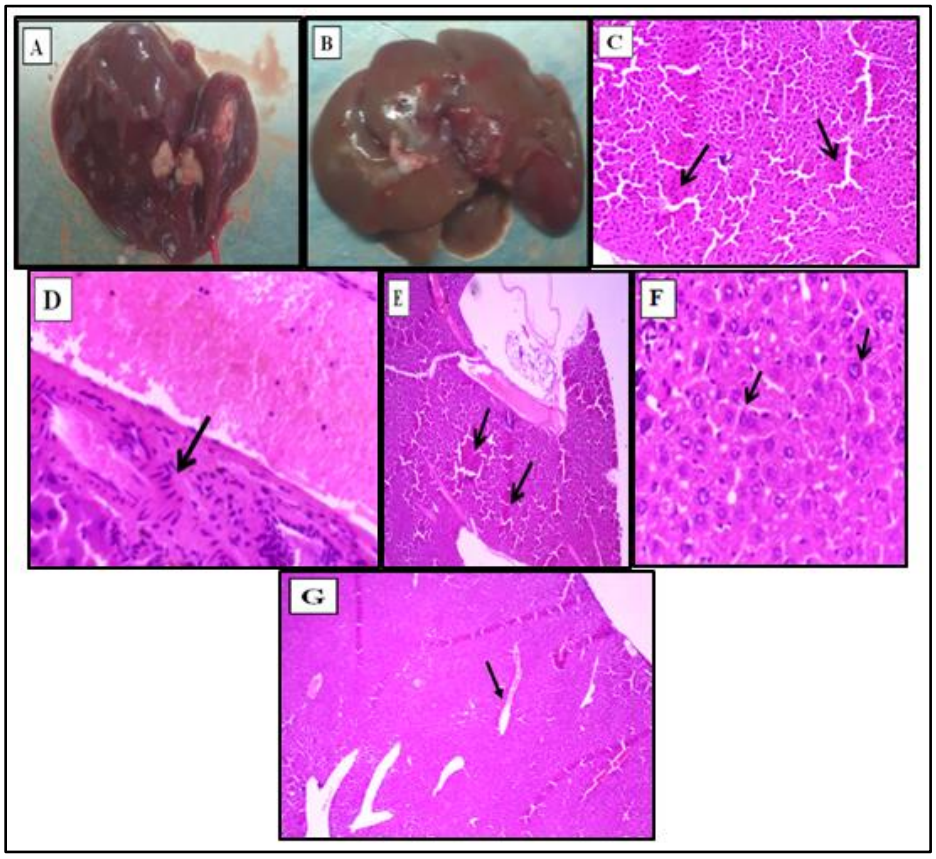

Figure 5.1: (A) Liver of the mice treated with saponins. (B) Liver of the non-treated mice. (C) Histopathology of liver showing marked portal tract inflammation. (D) Histopathology of liver depicting mildly dysplastic hepatocytes. (E) Histopathology showing congestion of sinuses. (F) Histopathology depicting lymphocyte infiltration in the portal tract. (G) Histopathology showing dilated vascular channels.

The abundance of lymphocytes in the portal tracts reflects significant inflammation as lymphocytes predominantly occur in the inflamed tissue. The histopathologies have confirmed that neither the plant extract saponins nor the time heals the inflamed liver (Figure 5.1). The liver injury induced by CCl_4 and ethanol remains irreversible in a time of seven weeks with saponin treatment or without treatment.

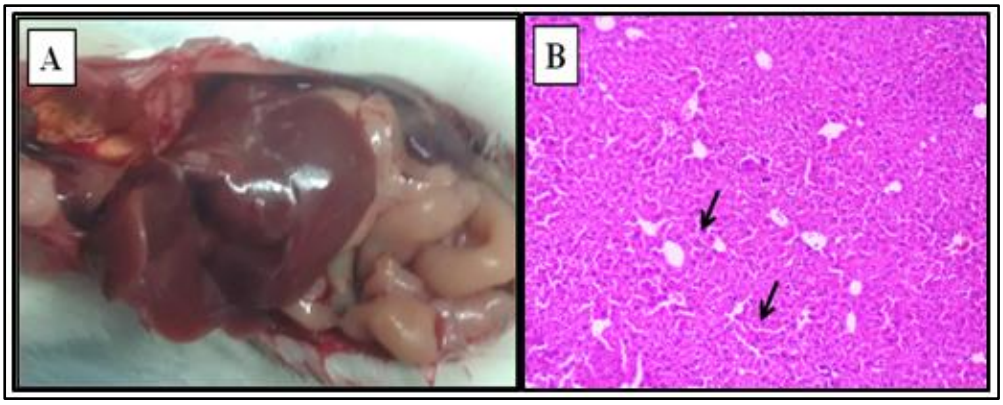

Figure 5.2: (A) The liver of mice treated with SapAuNps. (B) The histopathology after seven weeks of treatment with SapAuNps shows marked reduction in inflammation.

The histopathologies have confirmed that SapAuNps have successfully reduced liver inflammation over a period of seven weeks, mild portal tract inflammation and mild areas of congestion are apparent. The congestion of sinuses has been partially decreased. The vascular channels are not dilated anymore indicating potential efficiency of SapAuNps in recovering vasodilation.

5.2 Recovery of Spleen with or without Treatment

The spleen samples from all the three mice groups have revealed significant results. The spleen of saponin treated mice was markedly reduced in weight in comparison to the non-treated and AuNp treated mice, however the histopathologies of all the three mice groups are identical with slight differences, such as the histopathology of spleen sample of AuNps treated mice reveals mild inflammation. The histopathologies of the other two groups depict moderate inflammation and increased megakaryocyte infiltration.

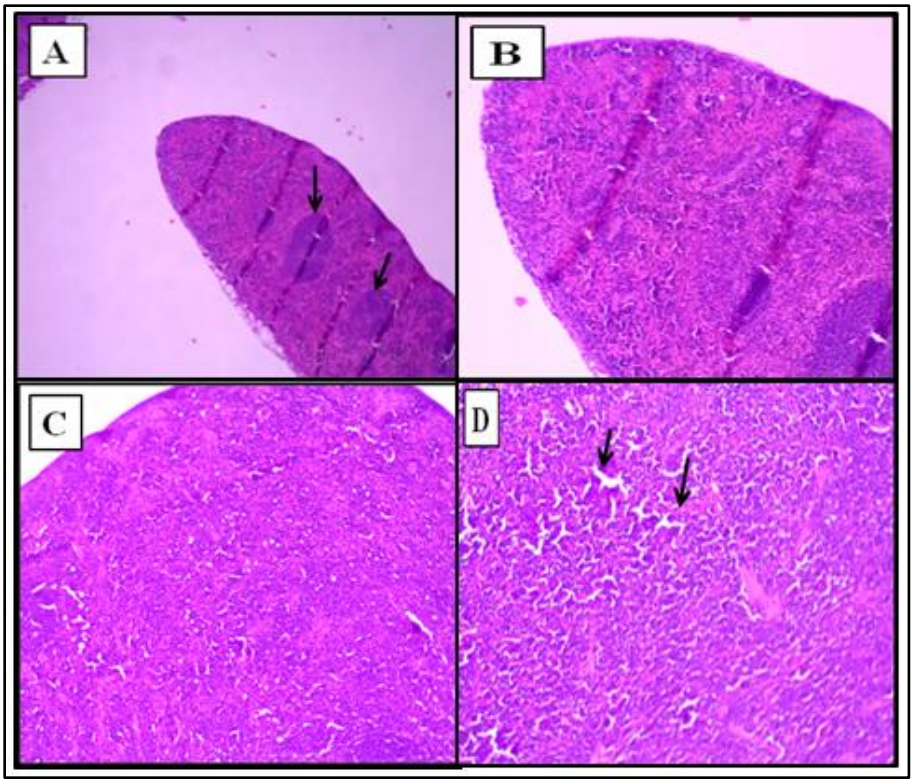

Figure 5.3: (A) Megakaryocytes are prominent and slightly increased in number in the splenic tissue of saponin treated and non-treated mice. (B) Shows the red and white pulp in the spleen tissue. (C) Mild portal tract inflammation in the splenic tissue of SapAuNps treated mice. (D) Moderate portal tract inflammation in the saponin treated and non-treated mice.

5.3 Effect of Treatment on Kidneys

The kidneys of mice treated with saponins appear normal upon dissection and are confirmed by histopathology to be normal, however the kidneys of the mice treated with SapAuNps appeared inflamed upon dissection and unremarkable renal tissue was reported by the histopathology (Figure 5.4).

It can be assumed that the tissue appear unremarkable due to severe inflammation as the repeated administration of AuNps is reported to cause accumulation of gold in the tissues reflecting tissue uptake (Lasagna-Reeves et al., 2010). Although gold nanoparticles improved the condition of the liver yet the effect of gold on the kidneys remained significant even in nanomolar concentrations (Higby, 1982) .

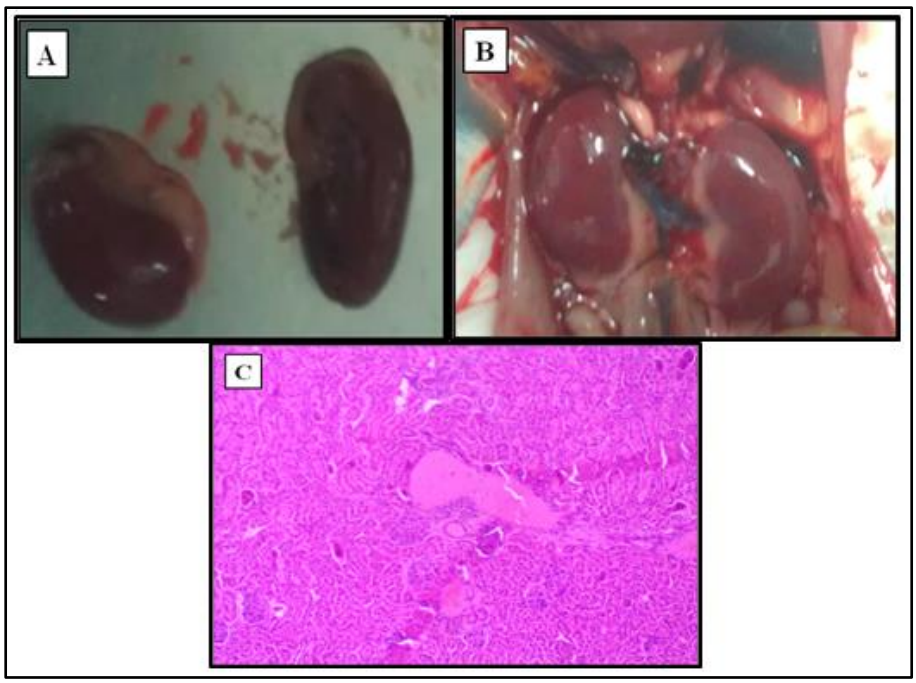

Figure 5.4: (A) Kidneys of the saponin treated mice. (B) Kidneys of the SapAuNps treated mice. (C) Histopathology of the inflamed kidney showing normal renal tissue.

CHAPTER 6: CONCLUSION

The intraperitoneal administration of 1µl/g of CCl_4 and Paraffin oil (50%v/v) in female Balb/c mice takes approximately 13 weeks to induce moderate liver inflammation. The change in the body weights of mice indicates the extent of liver damage. With the repeated administration of the toxin the faeces become watery and light brown. The body weights drop drastically in the last 12^{th} /13^{th} week and the mice become extremely weak and lethargic. Oral administration of ethanol via drinking water (5%v/v) makes the mice addicted/alcoholic, the mice drink more water and consume less food and have a pronounced sleep even in the light hours. In addition to the weight change splenomegaly is another potent indicator of severe liver damage. The aggressive behavior upon administration of the toxin and drowsiness upon alcohol intake are some of the symptoms of deteriorating health of mice.

The SapAuNps cannot be synthesized using methanol as a reference solvent as it tends to evaporate upon stirring. Moreover effective SapAuNps cannot be synthesized using volume of gold solutions in multiples other than the multiples of five. The saponin solution of 1mg/ml of deionized water is effective in synthesizing SapAuNps at Sap/Au ratios 2:1 and 6:1, keeping the concentration of gold solution constant. Small sized, spherical and monodispersed SapAuNps are synthesized by keeping higher gold salt solution concentrations such as 0.8mM and 1mM and lower saponin/gold ratios 2:1 and 6:1 respectively.

Gold nanoparticles of saponins are better in combating liver inflammation in comparison to the purified saponins. Moreover, the histopathologies of the non-treated mice further strengthened the hypothesis that liver inflammation remains irreversible for a period of seven weeks in the absence of treatment. SapAuNps effectively reduce inflammation within seven weeks but leave a side effect on the kidney which is histopathologically proven to be unharmful. In addition to the anti-inflammatory effect on the liver the SapAuNps also have a remarkable effect on the inflamed spleen. The results of the study support the hypothesis that saponin gold nanoparticles are pharmaceutically effective anti-inflammatory and anti-angiogenic agents.

REFERENCES

Abbasi, Tasneem, Anuradha, J, & Abbasi, SA. (2014). Utilization of the terrestrial weed guduchi (Tinospora cordifolia) in clean-green synthesis of gold nanoparticles. *Nanosci Technol, 1*(3), 1-7.

Abbate, Mauro, Zoja, Carla, Corna, Daniela, Rottoli, Daniela, Zanchi, Cristina, Azzollini, Nadia, . . . Morigi, Marina. (2008). Complement-mediated dysfunction of glomerular filtration barrier accelerates progressive renal injury. *Journal of the American Society of Nephrology, 19*(6), 1158-1167.

Ackermann, Daniel, Mordasini, David, Cheval, Lydie, Imbert-Teboul, Martine, Vogt, Bruno, & Doucet, Alain. (2007). Sodium retention and ascites formation in a cholestatic mice model: role of aldosterone and mineralocorticoid receptor? *Hepatology, 46*(1), 173-179.

Adinolfi, Luigi E, Gambardella, Michele, Andreana, Augusto, Tripodi, Marie-françoise, Utili, Riccardo, & Ruggiero, Giuseppe. (2001). Steatosis accelerates the progression of liver damage of chronic hepatitis C patients and correlates with specific HCV genotype and visceral obesity. *Hepatology, 33*(6), 1358-1364.

Alanazi, Fars K, Radwan, Awwad A, & Alsarra, Ibrahim A. (2010). Biopharmaceutical applications of nanogold. *Saudi Pharmaceutical Journal, 18*(4), 179-193.

Albano, Emanuele, & Vidali, Matteo. (2010). Immune mechanisms in alcoholic liver disease. *Genes & nutrition, 5*(2), 141-147.

Alivisatos, Paul. (2004). The use of nanocrystals in biological detection. *Nature biotechnology, 22*(1), 47-52.

Amendola, Vincenzo, & Meneghetti, Moreno. (2009). Size evaluation of gold nanoparticles by UV− vis spectroscopy. *The Journal of Physical Chemistry C, 113*(11), 4277-4285.

Amjadi, Mohammad, & Farzampour, Leila. (2014). Fluorescence quenching of fluoroquinolones by gold nanoparticles with different sizes and its analytical application. *Journal of Luminescence, 145*, 263-268.

Argentieri, Maria Pia, D'Addabbo, Trifone, Tava, Aldo, Agostinelli, Augusta, Jurzysta, Marian, & Avato, Pinarosa. (2008). Evaluation of nematicidal properties of saponins from Medicago spp. *European Journal of Plant Pathology, 120*(2), 189-197.

Arteel, Gavin E. (2011). Animal models of alcoholic liver disease. *Digestive Diseases, 28*(6), 729-736.

Batey, Robert G, Cao, Qi, & Gould, Belinda. (2002). Lymphocyte-mediated liver injury in alcohol-related hepatitis. *Alcohol, 27*(1), 37-41.

Bora, Parul. (2014). Anti-nutritional factors in foods and their effects. *Journal of Academia and Industrial Research, 3*(6), 285-290.

Böttger, Stefan, & Melzig, Matthias F. (2013). The influence of saponins on cell membrane cholesterol. *Bioorganic & medicinal chemistry, 21*(22), 7118-7124.

Brandon-Warner, Elizabeth, Schrum, Laura W, Schmidt, C Max, & McKillop, Iain H. (2012). Rodent models of alcoholic liver disease: of mice and men. *Alcohol, 46*(8), 715-725.

Burda, Clemens, Chen, Xiaobo, Narayanan, Radha, & El-Sayed, Mostafa A. (2005). Chemistry and properties of nanocrystals of different shapes. *Chemical reviews, 105*(4), 1025-1102.

Caldwell, Stephen H, & Crespo, Deborah M. (2004). The spectrum expanded: cryptogenic cirrhosis and the natural history of non-alcoholic fatty liver diseasePowell EE, Cooksley WGE, Hanson R, Searle J, Halliday JW, Powell LW. The natural history of nonalcoholic steatohepatitis: a follow-up study of forty-two patients for up to 21 years [Hepatology 1990; 11: 74–80]. *Journal of hepatology, 40*(4), 578-584.

Castera, L, Hezode, C, Roudot-Thoraval, F, Bastie, A, Zafrani, ES, Pawlotsky, JM, & Dhumeaux, D. (2003). Worsening of steatosis is an independent factor of fibrosis progression in untreated patients with chronic hepatitis C and paired liver biopsies. *Gut, 52*(2), 288-292.

Chang, Ming-Ling, Yeh, Chau-Ting, Chang, Pei-Yeh, & Chen, Jeng-Chang. (2005). Comparison of murine cirrhosis models induced by hepatotoxin administration and common bile duct ligation. *World journal of gastroenterology: WJG, 11*(27), 4167.

Day, Christopher P, & James, Oliver FW. (1998). Hepatic steatosis: innocent bystander or guilty party? *Hepatology, 27*(6), 1463-1466.

Ding, Wen–Xing, Li, Min, Chen, Xiaoyun, Ni, Hong–Min, Lin, Chih–Wen, Gao, Wentao, . . . Yin, Xiao–Ming. (2010). Autophagy reduces acute ethanol-induced hepatotoxicity and steatosis in mice. *Gastroenterology, 139*(5), 1740-1752.

Domenicali, Marco, Caraceni, Paolo, Giannone, Ferdinando, Baldassarre, Maurizio, Lucchetti, Giovanna, Quarta, Carmelo, . . . Lemoli, Roberto M. (2009). A novel model of CCl 4-induced cirrhosis with ascites in the mouse. *Journal of hepatology, 51*(6), 991-999.

Friedman, Scott L. (2008). Hepatic stellate cells: protean, multifunctional, and enigmatic cells of the liver. *Physiological reviews, 88*(1), 125-172.

Gadelha, Ivana Cristina Nunes, Câmara, Antônio Carlos Lopes, Pacífico-da-Silva, Idalécio, Batista, Jael Soares, Melo, Marília Martins, & Soto-Blanco, Benito. (2015). Toxic Effects of the Pericarp of the Enterolobium contortisiliquum (Vell.) Morong Fruit on Chicks. *International Journal of Applied Research in Veterinary, 13*, 135.

Ganeshkumar, Moorthy, Sastry, Thotapalli Parvathaleswara, Kumar, Muniram Sathish, Dinesh, Murugan Girija, Kannappan, Sudalyandi, & Suguna, Lonchin. (2012). Sun light mediated synthesis of gold nanoparticles as carrier for 6-mercaptopurine: Preparation, characterization and toxicity studies in zebrafish embryo model. *Materials Research Bulletin, 47*(9), 2113-2119.

Gengatharan, Ashwini, Dykes, Gary A, & Choo, Wee Sim. (2015). Betalains: natural plant pigments with potential application in functional foods. *LWT-Food Science and Technology, 64*(2), 645-649.

Ghosh, Partha, Han, Gang, De, Mrinmoy, Kim, Chae Kyu, & Rotello, Vincent M. (2008). Gold nanoparticles in delivery applications. *Advanced drug delivery reviews, 60*(11), 1307-1315.

Giljohann, David A, Seferos, Dwight S, Daniel, Weston L, Massich, Matthew D, Patel, Pinal C, & Mirkin, Chad A. (2010). Gold nanoparticles for biology and medicine. *Angewandte Chemie International Edition, 49*(19), 3280-3294.

Golemanov, Konstantin, Tcholakova, Slavka, Denkov, Nikolai, Pelan, Eddie, & Stoyanov, Simeon D. (2014). The role of the hydrophobic phase in the unique rheological properties of saponin adsorption layers. *Soft Matter, 10*(36), 7034-7044.

Gressner, AM, & Weiskirchen, R. (2006). Modern pathogenetic concepts of liver fibrosis suggest stellate cells and TGF-β as major players and therapeutic targets. *Journal of cellular and molecular medicine, 10*(1), 76-99.

Güçlü-Üstündağ, Özlem, & Mazza, Giuseppe. (2007). Saponins: properties, applications and processing. *Critical reviews in food science and nutrition, 47*(3), 231-258.

Guo, Qingquan, Guo, Qiulan, Yuan, Juan, & Zeng, Jinhua. (2014). Biosynthesis of gold nanoparticles using a kind of flavonol: Dihydromyricetin. *Colloids and Surfaces A: Physicochemical and Engineering Aspects, 441*, 127-132.

Han, Derick, Ybanez, Maria D, Johnson, Heather S, McDonald, Jeniece N, Mesropyan, Lusine, Sancheti, Harsh, . . . Dara, Lily. (2012). Dynamic Adaptation of Liver Mitochondria to Chronic Alcohol Feeding in Mice BIOGENESIS, REMODELING, AND FUNCTIONAL ALTERATIONS. *Journal of Biological Chemistry, 287*(50), 42165-42179.

Hickman, IJ, Clouston, AD, Macdonald, GA, Purdie, DM, Prins, JB, Ash, S, . . . Powell, EE. (2002). Effect of weight reduction on liver histology and biochemistry in patients with chronic hepatitis C. *Gut, 51*(1), 89-94.

Higby, Gregory J. (1982). Gold in medicine. *Gold bulletin, 15*(4), 130-140.

Hooijmans, Carlijn R, Leenaars, Marlies, & Ritskes-Hoitinga, Merel. (2010). A gold standard publication checklist to improve the quality of animal studies, to fully integrate the Three Rs, and to make systematic reviews more feasible.

Hostettmann, Kurt, & Marston, Andrew. (2005). *Saponins*: Cambridge University Press.

Järveläinen, Harri A, Fang, Che, Ingelman-Sundberg, Magnus, & Lindros, Kai O. (1999). Effect of chronic coadministration of endotoxin and ethanol on rat liver pathology and proinflammatory and anti-inflammatory cytokines. *Hepatology, 29*(5), 1503-1510.

Khanal, Tilak, Choi, Jae Ho, Hwang, Yong Pil, Chung, Young Chul, & Jeong, Hye Gwang. (2009). Saponins isolated from the root of Platycodon grandiflorum protect against acute ethanol-induced hepatotoxicity in mice. *Food and chemical toxicology, 47*(3), 530-535.

Kim, Dongkyu, & Jon, Sangyong. (2012). Gold nanoparticles in image-guided cancer therapy. *Inorganica Chimica Acta, 393*, 154-164.

Kita, Hiroto, Van De Water, Judy, Gershwin, M Eric, & Mackay, Ian R. (2001). The lymphoid liver: considerations on pathways to autoimmune injury. *Gastroenterology, 120*(6), 1485-1501.

Korpassy, B, & Kovacs, K. (1949). Experimental liver cirrhosis in rats, produced by prolonged subcutaneous administration of solutions of tannic acid. *British journal of experimental pathology, 30*(4), 266.

Lan, Ming-Ying, Hsu, Yen-Bin, Hsu, Chih-Hung, Ho, Ching-Yin, Lin, Jin-Ching, & Lee, Sheng-Wei. (2013). Induction of apoptosis by high-dose gold nanoparticles in nasopharyngeal carcinoma cells. *Auris Nasus Larynx, 40*(6), 563-568.

Lasagna-Reeves, C, Gonzalez-Romero, D, Barria, MA, Olmedo, I, Clos, A, Ramanujam, VM Sadagopa, . . . Soto, C. (2010). Bioaccumulation and toxicity of gold nanoparticles after repeated administration in mice. *Biochemical and biophysical research communications, 393*(4), 649-655.

Li, Yuchang, Wang, Jiaohong, & Asahina, Kinji. (2013). Mesothelial cells give rise to hepatic stellate cells and myofibroblasts via mesothelial–mesenchymal transition in liver injury. *Proceedings of the National Academy of Sciences, 110*(6), 2324-2329.

Liedtke, Christian, Luedde, Tom, Sauerbruch, Tilman, Scholten, David, Streetz, Konrad, Tacke, Frank, . . . Weiskirchen, Ralf. (2013). Experimental liver fibrosis research: update on animal models, legal issues and translational aspects. *Fibrogenesis & tissue repair, 6*(1), 19.

Lonardo, Amedeo, Adinolfi, Luigi E, Loria, Paola, Carulli, Nicola, Ruggiero, Giuseppe, & Day, Christopher P. (2004). Steatosis and hepatitis C virus: mechanisms and significance for hepatic and extrahepatic disease. *Gastroenterology, 126*(2), 586-597.

Lorent, Joseph H, Quetin-Leclercq, Joëlle, & Mingeot-Leclercq, Marie-Paule. (2014). The amphiphilic nature of saponins and their effects on artificial and biological membranes and potential consequences for red blood and cancer cells. *Organic & biomolecular chemistry, 12*(44), 8803-8822.

Man, Shuli, Gao, Wenyuan, Zhang, Yanjun, Huang, Luqi, & Liu, Changxiao. (2010). Chemical study and medical application of saponins as anti-cancer agents. *Fitoterapia, 81*(7), 703-714.

McLean, Elizabeth K, McLean, AEM, & Sutton, PM. (1969). Instant cirrhosis: an improved method for producing cirrhosis of the liver in rats by simultaneous administration of carbon tetrachloride and phenobarbitone. *British journal of experimental pathology, 50*(5), 502.

Mohadesi, Alireza, Ranjbar, Mehdi, & Salmanipour, Ashraf. (2016). Synthesis and characterization of gold nanoparticles with the aid of green reducing agent through the free surfactant microwave method. *Journal of Materials Science: Materials in Electronics, 27*(9), 9073-9077.

Moriya, Kyoji, Fujie, Hajime, Shintani, Yoshizumi, Yotsuyanagi, Hiroshi, Tsutsumi, Takeya, Ishibashi, Kotaro, . . . Koike, Kazuhiko. (1998). The core protein of hepatitis C virus induces hepatocellular carcinoma in transgenic mice. *Nature medicine, 4*(9), 1065-1067.

Oleszek, Wieslaw, & Marston, Andrew. (2013). *Saponins in food, feedstuffs and medicinal plants* (Vol. 45): Springer Science & Business Media.

Ozturk, Bengu, & McClements, David Julian. (2016). Progress in natural emulsifiers for utilization in food emulsions. *Current Opinion in Food Science, 7*, 1-6.

Pal, Rajat, Panigrahi, Swati, Bhattacharyya, Dhananjay, & Chakraborti, Abhay Sankar. (2013). Characterization of citrate capped gold nanoparticle-quercetin complex: Experimental and quantum chemical approach. *Journal of Molecular Structure, 1046*, 153-163.

Pessayre, Dominique, & Fromenty, Bernard. (2005). NASH: a mitochondrial disease. *Journal of hepatology, 42*(6), 928-940.

Pissuwan, Dakrong, Valenzuela, Stella M, & Cortie, Michael B. (2006). Therapeutic possibilities of plasmonically heated gold nanoparticles. *TRENDS in Biotechnology, 24*(2), 62-67.

Powell, Elizabeth E, Jonsson, Julie R, & Clouston, Andrew D. (2005). Steatosis: co-factor in other liver diseases. *Hepatology, 42*(1), 5-13.

Raghavendra, R, ARUNACHALAM, KANTHADEIVI, ANNAMALAI, SATHESH KUMAR, & AARRTHY, M. (2014). Diagnostics and therapeutic application of gold nanoparticles. *medicine (bio diagnostics, drug delivery and cancer therapy), 2*, 4.

Ribeiro, Bernardo Dias, Alviano, Daniela Sales, Barreto, Daniel Weingart, & Coelho, Maria Alice Zarur. (2013). Functional properties of saponins from sisal (Agave sisalana) and juá (Ziziphus joazeiro): critical micellar concentration, antioxidant and antimicrobial activities. *Colloids and Surfaces A: Physicochemical and Engineering Aspects, 436*, 736-743.

Rosarin, F Stanley, & Mirunalini, S. (2011). Nobel metallic nanoparticles with novel biomedical properties. *Journal of Bioanalysis & Biomedicine, 2011*.

Sadeghi, Babak. (2015). Zizyphus mauritiana extract-mediated green and rapid synthesis of gold nanoparticles and its antibacterial activity. *Journal of Nanostructure in Chemistry, 5*(3), 265-273.

Sequoia Ecosystem and Recreation Preserve Act of 1999, H.R.2077, U.S. House of Representatives (1999).

Shankar, S Shiv, Rai, Akhilesh, Ahmad, Absar, & Sastry, Murali. (2005). Controlling the optical properties of lemongrass extract synthesized gold nanotriangles and potential application in infrared-absorbing optical coatings. *Chemistry of Materials, 17*(3), 566-572.

Sparg, SG , Light, ME, & Van Staden, J. (2004). Biological activities and distribution of plant saponins. *Journal of ethnopharmacology, 94*(2), 219-243.

Srivastava, AK, Yadev, Rishikesh, Rai, VN, Ganguly, Tapas, & Deb, SK. (2012). *Surface plasmon resonance in gold nanoparticles.* Paper presented at the AIP Conference Proceedings.

Stobiecka, Magdalena, & Hepel, Maria. (2011). Double-shell gold nanoparticle-based DNA-carriers with poly-L-lysine binding surface. *Biomaterials, 32*(12), 3312-3321.

Thakur, Mayank, Jerz, Gerold, Tuwalska, Dorota, Gilabert-Oriol, Roger, Wybraniec, Sławomir, Winterhalter, Peter, . . . Weng, Alexander. (2014). High-speed countercurrent chromatographic recovery and off-line electrospray ionization mass spectrometry profiling of bisdesmodic saponins from Saponaria officinalis possessing synergistic toxicity enhancing properties on targeted antitumor toxins. *Journal of Chromatography B, 955*, 1-9.

Vasina, Valentina, Giannone, Ferdinando, Domenicali, Marco, Latorre, Rocco, Berzigotti, Annalisa, Caraceni, Paolo, . . . Bernardi, Mauro. (2012). Portal hypertension and liver cirrhosis in rats: effect of the β3-adrenoceptor agonist SR58611A. *British journal of pharmacology, 167*(5), 1137-1147.

Vincken, Jean-Paul, Heng, Lynn, de Groot, Aede, & Gruppen, Harry. (2007). Saponins, classification and occurrence in the plant kingdom. *Phytochemistry, 68*(3), 275-297.

Waller, George R, & Yamasaki, Kazuo. (2013). *Saponins used in traditional and modern medicine* (Vol. 404): Springer Science & Business Media.

Walsh, Meagan J, Vanags, Daina M, Clouston, Andrew D, Richardson, Michelle M, Purdie, David M, Jonsson, Julie R, & Powell, Elizabeth E. (2004). Steatosis and liver cell apoptosis in chronic hepatitis C: a mechanism for increased liver injury. *Hepatology, 39*(5), 1230-1238.

Westin, Johan, Nordlinder, Hans, Lagging, Martin, Norkrans, Gunnar, & Wejstål, Rune. (2002). Steatosis accelerates fibrosis development over time in hepatitis C virus genotype 3 infected patients. *Journal of hepatology, 37*(6), 837-842.

Wulf, Ashley. (2012). *Determining the Size and Shape of Gold Nanoparticles.*

Wyatt, J, Baker, H, Prasad, P, Gong, YY, & Millson, C. (2004). Steatosis and fibrosis in patients with chronic hepatitis C. *Journal of clinical pathology, 57*(4), 402-406.

Yip, William W, & Burt, Alastair D. (2006). *Alcoholic liver disease.* Paper presented at the Seminars in diagnostic pathology.

Zabetakis, Kara, Ghann, William E, Kumar, Sanjeev, & Daniel, Marie-Christine. (2012). Effect of high gold salt concentrations on the size and polydispersity of gold nanoparticles prepared by an extended Turkevich–Frens method. *Gold Bulletin, 45*(4), 203-211.

Zatloukal, Kurt, Stumptner, Conny, Fuchsbichler, Andrea, Fickert, Peter, Lackner, Carolin, Trauner, Michael, & Denk, Helmut. (2004). The keratin cytoskeleton in liver diseases. *The Journal of pathology, 204*(4), 367-376.

Zeisberg, Michael, Yang, Changqing, Martino, Margot, Duncan, Michael B, Rieder, Florian, Tanjore, Harikrishna, & Kalluri, Raghu. (2007). Fibroblasts derive from hepatocytes in liver fibrosis via epithelial to mesenchymal transition. *Journal of Biological Chemistry, 282*(32), 23337-23347.